AIR FORCE INSTITUTE OF TECHNOLOGY

AIR UNIVERSITY
UNITED STATES AIR FORCE

SCHOOL OF ENGINEERING

WRIGHT-PATTERSON AIR FORCE BASE, OHIO

AF-WP-O-MAY 62 3,500

THE ANALYSIS, OPTIMIZATION, AND DESIGN OF AN AIRBORNE RADIATION SAMPLING ELECTROSTATIC PRECIPITATOR

THESIS

GNE-62

Robert Stanley Stuart
Lt USAF

AF-WP-O-AUG 62 22

THE ANALYSIS, OPTIMIZATION, AND DESIGN OF AN AIRBORNE RADIATION SAMPLING ELECTROSTATIC PRECIPITATOR

THESIS

Presented to the Faculty of the School of Engineering of
the Institute of Technology
Air University
in Partial Fulfillment of the
Requirements for the Degree of
Master of Science

By

Robert Stanley Stuart, B.S. A.E.

Lt USAF

Graduate Nuclear Engineering

May 1962

Preface

I have attempted in this report to present the results of my studies over the past few months on the use of electrostatic precipitation as a method of collecting airborne radioactive aerosols. I sincerely hope the results contained herein will prove useful to those who share my enthusiasm for this subject. The usefulness of this thesis, then, will be in the utilization of the optimization theory presented, which will precede an actual design, and the designers ability to successfully predict the results he might expect from such a design. Fortran computer symbols are used throughout this study in the hope the computer program presented in the appendices will be easily understood.

I am greatly in debt to my thesis advisor, Capt. Charles J. Bridgman, who not only initially aroused my interest in this subject, but who also has provided the guidance and incentive necessary to successfully complete this work. Similarly, the aid of Wayne Buchtel and Capt. Bridgman concerning the digital computer program is greatly acknowledged. Although the assistance of the aforementioned has been freely used, the responsibility for errors rests solely with me.

Finally, this work could not have been completed without the aid and inspiration of my wife. Not only has she provided sunshine for the dark hours, but also throughout this entire study she has generously displayed virtues of faith, hope, and charity.

Robert S. Stuart

Contents

Contents

Contents

List of Figures

List of Tables

List of Symbols

Symbol	
AREA	Area of wire frame holding the corona wires (cm^2).
CUN(J)	Cunningham correction factor for a particle in size group J (dimensionless).
CUR	Corona current acting between the corona wires and one plate (amps).
DA	Distance traveled by a particle toward the collection section anode (am).
DAC	Distance traveled by a particle toward the charging section anode (am).
DCH	Length of charging section (cm).
DL	Length of collection section (cm).
E	Effective ionization field (volts/cm).
ECOL	Electric field in the collection section (volts/cm).
EFF	Precipitator efficiency (dimensionless).
FC	Fraction of the particles leaving the charging section that are collected in the collection section (dimensionless).
FCC	Fraction of particles collected in the charging section (dimensionless).
FQQ	Fraction of bombardment saturation charge achieved by an aerosol in time T (dimensionless).
FRAR	Precipitator frontal area, less frontal area of plates (cm^2).
FR(J)	Mass fraction of a particle in size group J (dimensionless).
FRTO	Total fraction collected (dimensionless).
G	Ion density ($ions/cm^3$).
I	Total corona current (amps).
J	Particle size group (dimensionless).

List of Symbols

G(I)	Charge at any time T (electrons).
QP	Time rate of change of charge dq/dt (electrons/sec).
QQ	Charge achieved by an aerosol as it enters the collection section (electrons).
R(J)	Radius of a particle of size group J (cm).
SEN	Sensitivity of the precipitator (m^3/min).
SEP	Plate separation in the collection section (cm).
SEPC	Plate separation in the charging section (cm).
T	Time spent by the aerosol in the charging section (sec).
u	Micron (10^{-4} cm).
VD	Drift velocity of the aerosol toward the anode in the collection section (cm/sec).
V(I)	Velocity at any time T of an aerosol toward the anode in the charging section (cm/sec).
VL	Velocity of air flow thru the charging section (cm/sec).
VLCL	Velocity of air flow thru the collection section (cm/sec).
VOL	Volume flow of air thru the precipitator (m^3/min).
	Kinematic viscosity (ft^2/sec).

Abstract

The analysis, optimization, and design of a two-stage parallel plate precipitator are discussed. An IBM 7090 digital computer program is used to achieve all theoretical results. Negative corona discharge is used throughout, and aerosol charging by bombardment and diffusion methods are combined into one time dependent equation. Precipitator optimization theory is presented and the effects on precipitator sensitivity and efficiency of varying corona current, velocity, and geometry are studied in detail. A theoretical design is presented in order to determine the feasibility of precipitation at high velocities and altitudes.

GNE/PHYS/62-16

THE ANALYSIS, OPTIMIZATION, AND DESIGN OF AN AIRBORNE RADIATION SAMPLING ELECTROSTATIC PRECIPITATOR

I. Introduction

The purpose of this thesis is to theoretically predict, analyze, and attempt to optimize the results of a precipitator that has already been designed, and to present a design of a precipitator to be tested in a high speed wind tunnel. An aerosol, for the purpose of this thesis, is a particle suspended in the atmosphere. The particles under consideration are those to which long-lived fission products resulting from a nuclear explosion, reactor accident, or nuclear rocket launch, have become attached.

The importance of knowing the amount of radioactivity present in the atmosphere as a result of the above is paramount. Since the particle density (number of particles/m^3) is low except immediately after an explosion or accident, a device is required that has a high rate (particles/min) of collection. Collection devices generally used today are of the filter type, and boast of a high collection efficiency (fraction of particles collected). Although filters have a high efficiency (almost 100%), they cannot sustain high flow rates and therefore cannot collect a large number of particles in a short time. The flow rate through a filter system depends upon the type of filter used, and decreases throughout the filtration process as the collected particles become attached to the filter. A device is needed that will not only

have a high efficiency, but can also sustain a high flow rate and therefore collect a large number of particles in a short time. Since the statistics of counting a large sample of radioactive material is much better than that of a small sample, the amount of particles collected is the most important goal to try to achieve in radioactive aerosol collection. The sensitivity of the precipitator is a measure of this goal and is defined as

$$SEN = (EFF)(VOL) \tag{1}$$

where SEN is the sensitivity of the precipitator in m^3/min, EFF is the total efficiency of the precipitator, and VOL is the volume flow of air thru the precipitator in m^3/min.

One can easily see from Eq (1) that a high sensitivity can be achieved with a relatively low efficiency if the volume flow of air is high. Since the filters in use today are made of a thin porous material, they cannot sustain large flow rates. The strength of the filter places an upper limit on the flow rate it can sustain, which in turn sets an upper limit on the sensitivity that the filter system can achieve. Present day filters can sustain flow rates of around 1.5 m^3/min. A machine that is to replace the filter as a means of collecting radioactive samples should be capable of greatly exceeding this figure, be as compact as possible, and should cost as little as possible. The electrostatic precipitator has little or no restriction on the volume flow of air it can sustain.

In the application of an electrostatic precipitator as a means of collecting radioactive samples, the sensitivity of the machine is

is affected by a variety of parameters that may be adjusted while the machine is in the design stages, and a few that may be adjusted after the machine has been designed and is in operation. The problem therefore, is to adjust these parameters to achieve a maximum sensitivity so as to justify the use of a precipitator as a means of collection.

Electrostatic precipitators have long been used as a means of collecting dirt and ashes from the air. Their value as a means of sampling the air for radioactivity is forthcoming, and even further use for the precipitator in the nuclear field requires only a small amount of imagination.

The scope of this thesis is not intended to include a long detailed presentation of the electric theory governing electrostatic precipitators, but rather to apply the theory in an orderly fashion so that the effects of the various parameters might be better understood. Although considerable background information on the theory involved is presented; a complete precipitator analysis, optimization, and design are the principle goals of this study. This not only provides an example by which other precipitators may be compared, but should also be of significant use in designing future precipitators and predicting the results that may be expected from their use. The theory concerned with the optimization of a precipitator is presented seperately in the chapter dealing with precipitator optimization.

This thesis is conveniently divided into sub-areas. These sub-areas of investigation will be discussed in the order given. First, a complete theoretical analysis will be presented on the performance of a two stage parallel plate precipitator (named EARC I) that is now

in use collecting radioactive aerosol samples at the Air Force Institute of Technology. Conclusions and recommendations for improving its performance will also be presented. The theoretical predictions will be compared to the experimental results. Second, a study of the effects of varying the parameters on this machine will be presented, leading toward an optimum design within set design limits. This sub-area will in turn lead to a theoretical design intended to achieve maximum performance from limited materials and equipment available. Third, the results of the first two sub-areas will be used to formulate a preliminary design of an electrostatic precipitator to be tested in a high speed wind tunnel in order to determine the feasibility of operating a precipitator at high velocities and altitudes. Finally, the conclusions of this study are presented as items of design philosophy.

The reader will note that Fortran computer symbols are used in the equations throughout the entire study. It is hoped that the use of such symbols will be of considerable help in aiding the reader understand the computer programs that are presented in Appendices A and B of this thesis.

II. Precipitator Theory

The purpose of this chapter is to present the theory involved in the electrostatic precipitator collection process. For the purpose of this thesis, only theory concerned with a two-stage parallel-plate precipitator will be presented. Optimization theory will be presented in the chapter concerned with the precipitator optimization process. The theory of two-stage precipitators is easily broken up into two processes, ionization and collection, each of which will be presented separately.

Aerosol Distribution Spectrum

Since the response of an aerosol to an electrostatic precipitator is particularly dependent upon the size of the aerosol, it is important that each size particle be treated separately in the precipitation process. The aerosols to be considered in this thesis will therefore be divided into size groups. Although the selection of the size groups is completely arbitrary, Lamberson (Ref 4:63) has conveniently divided the size spectrum of radioactive aerosols into twelve groups. This spectrum will be used throughout this study. In the distribution of group sizes, Lamberson makes several important assumptions (Ref 4:64). First, the assumption is made that the distribution spectrum under consideration is the mean distribution spectrum of long-lived fission products of stratospheric origin. That is to say, the radioactivity is homogeneously distributed with respect to aerosol volume and the radioactivity fraction in a group equals the volume fraction of the same group, which also equals

the mass fraction of that group (assuming constant density). Lamberson also assumes that the lower and upper limits of the distribution spectrum for long-lived fission products are 0.1 and 10.0 u radii respectively. Table I shows the twelve group distribution spectrum made on the above assumptions. As can be seen from Table I, the average radius of each group is calculated and this figure will be used as the representative radii for that group. The mass fraction is that fraction of the total mass of twelve groups that is representative of that group.

Ionization Section

The ionization section plays a very important role in the precipitation process. Although the aerosols may be charged by many different processes including x-rays, gamma rays, friction, flames, photo electricity, and various types of electrical discharge (Ref 10:1186); only charging by corona discharge will be considered in this thesis. Each of the above types of charging has proven inferior to corona discharge, so that the electrostatic precipitators in use today almost exclusively use the corona discharge to achieve particle charging.

The Need for Charge. Electrostatic precipitation is based entirely on the collection of charged particles. As will be shown later, the success of the precipitator is directly proportional to the amount of charge each individual aerosol achieves as it passes thru the ionization section. Therefore it is desirable to charge each particle as much as possible in order that it will be readily collected during the collection process.

Table I
Division of the Distribution Spectrum into Groups

Group	Particle Radius Range (u)	Ave Radius (u)	Mass Fraction
1	0.1 -0.15	.125	.0881
2	0.15-0.25	.200	.1109
3	0.25-0.35	.300	.0731
4	0.35-0.50	.425	.0774
5	0.50-0.70	.600	.0731
6	0.70-1.00	.850	.0774
7	1.00-1.50	1.250	.0881
8	1.50-2.50	2.000	.1109
9	2.50-3.50	3.000	.0731
10	3.50-5.00	4.250	.0774
11	5.00-7.00	6.000	.0731
12	7.00-10.0	8.500	.0774
			Σ 1.0000

Adapted from (Ref 4:63A)

Corona Discharge. When the uniform electric field (volts/cm) present between a pair of parallel plates exceeds a certain value (around 30 kv/cm in standard air), electrical breakdown of the gas, resulting in a sparkover takes place (Ref 8:32). Corona discharge can not take place in a uniform field. However with a wire and plate electrode system, such as that being considered in this study, the field distribution in the inter-electrode space is not uniform but varies from a high value at the wire to a low value at the plate surface (Ref 8:32). Application of a suitable potential difference between the wires and plate result in electrical breakdown of the gas close to the wire, due to the high field strength in this region. This condition which is accompanied by a blue glow surrounding the wire, constitutes the corona. A further increase in the applied voltage leads to complete breakdown of the gap, with complete sparkover. If this sparkover or "arcing" persists for any length of time the electrodes are in effect short-circuited and the precipitator ceases to operate. Therefore, for the successful operation of a precipitator it is necessary that a steady corona be maintained. High precipitator efficiency demands a high field strength. Therefore the applied voltage must be as high as possible to maintain a steady corona and must not be high enough to result in the arcing condition to take place.

There are two types of corona discharge available to the designer of an electrostatic precipitator depending on which electrode is grounded. If the wires are the cathode, the discharge is negative corona and the corona discharge glow will be visible near the wires.

With negative corona, there is a liberation of electrons from the wire by positive ion bombardment and by photo emission. The electrons, repelled from the wire by the field, quickly form negative ions by attachment to the air molecules which, in turn, move toward the anode and constitute a unipolar space charge. If the wires are the anode, the discharge is positive, and positive ions predominate in the gap (Ref 4:28). Since negative corona is more stable and allows higher operating currents and voltages than positive corona (Ref 10:1186-1187), all future reference to corona discharge in this study will refer only to negative corona.

Effective Ionization Field. The effective ionization field for purposes of this study is defined to be that electric field that is present between the wire and plate electrode system in the ionization section. The effective ionization field in a vertical plane containing a wire, and one midway between wires is not constant (Ref 4:65). However, since the distance between the cathode wires and between the cathode and anode is small for purposes of this study, the electric field is assumed to be linear. This assumption is made primarily because to date there is no analytical theory available to predict the potential distribution and its use probably presents no great error (Ref 4:28).

Ion Density. Under standard air conditions the ion density (ions/cm^3) can be calculated by (Ref 4:37):

$$G = 0.352 \times 10^{19} \frac{CUR}{(E)(AREA)} \qquad (2)$$

where CUR is the corona current in amperes, E is the effective electric

field in volts/cm, and AREA is the cathode area in cm^2.

The specific corona current is a function of wire material and diameter and is given by

$$CUR = (Z)(L) \tag{3}$$

where Z is a constant dependent on wire size and material in amps/cm and L is the length of wire discharging corona in cm. For purposes of this thesis Z will be a experimentally determined quantity using results obtained with EARC I as described in Chapter III.

The ion density is assumed homogeneous throughout the volume of the ionization section. This will be nearly true at all locations except very near the cathode wires. In this plane, as one progresses from the inlet to the outlet of the ionization section near a wire, the ion density would be alternately higher and lower (Ref 4:67). Therefore, this assumption is probably quite valid.

Aerosol Charging. Two distinctive charging processes account for the charge an aerosol achieves while it is in the ionization section. These processes are bombardment and diffusion charging respectively. Each process will be described seperately and an expression combining the two processes will be presented. Although both processes operate simultaneously, it can be shown that diffusion charging is important only for particles having a radius of less than about 0.3u (Ref 4:40). Since the size groups under consideration include particles of radii as small as 0.1u, diffusion charging must be considered.

In bombardment charging, the ions of the air, moving rapidly under the influence of the applied electric field, collide with the aerosols

and attach themselves to the aerosol surface. The charge achieved by each aerosol depends upon the strength of the charging field, surface area, dielectric properties of the aerosol, and the time the aerosol spends in the ionization section. The charge transferred to the aerosol establishes a repulsive force so that the next ion which strikes the aerosol must overcome this coulomb repulsion. Eventually sufficient charge is achieved by the particle to nullify the electric field, charging ceases, and the aerosol is said to have received a saturation charge. White lists three assumptions necessary to solve the problem (Ref 10:1187):

1. The aerosol particles are spherical.
2. Particle diameter is much less than the distance between particles.
3. The ion concentration and electric field are uniform in the immediate region surrounding a particle.

With ion diffusion charging the thermal motion of the ions cause diffusion through the gas, and the charging of the aerosols is effected irrespective of the presence of an electric field. The charge achieved by the aerosol in the diffusion process is dependent upon the size of the particle, the air temperature, and the time the aerosol spends in the charging section. The assumptions used by White to solve the problem are (Ref 10:1187-1189):

1. The particles are spherical.
2. Particle diameter is much less than the distance between particles.

3. The ion concentration and electric field are uniform in the immediate region surrounding a particle.

4. All ions which reach the particle are attached.

Making use of the above assumptions, Lamberson has derived the following expression for the combined bombardment and diffusion charging in the ionization section of a two-stage parallel-plate precipitator for air at 30 C (Ref 4:43):

$$\frac{dq}{dt} = A - Bq + Cq^2 + De^{-Fq} \tag{4}$$

where $A = 11.16GR^2E$

$B = 1.61 \times 10^{-6} G$

$C = 5.79 \times 10^{-14} \frac{G}{R^2E}$

$D = 15.7 \times 10^{+4} GR^2$

$F = \frac{+5.56 \times 10^{-6}}{R}$

and G is the ion density in ions/cm^3, R is the particle radius in cm, and E is the effective electric field in volts/cm.

Eq (4) is a non-linear differential equation to which there is no analytical solution. The first three terms on the right side indicate the effect of bombardment charging, while the last term accounts for diffusion charging. Appendix A shows Eulers numerical analysis method of solution (Ref 9:71) using a IBM 7090 digital computer.

Bombardment Saturation Charging. Since bombardment charging is the important charging mechanism for particles whose radius is greater than about 0.3 u , a useful measurement of the fraction of saturation

charge achieved by the particle by bombardment is given by Lamberson as (Ref 4:36):

$$FQQ = \frac{1}{1 + \frac{1}{2.23 \times 10^{-7}\ GT}} \tag{5}$$

where FQQ is the fraction of saturation charge achieved by bombardment, G is the ion density in ions/cm^3, and T is the time spent in the ionization section in seconds.

Fraction Collected in the Charging Section. Baker (Ref 1: Chapter III), has experimentally noted that a certain amount of particles are being collected in the ionization section, before entering the collection section. As the aerosols enter the ionization section they pick up charge almost instantaneously. The amount of charge increases as the particle passes thru the ionization section, the particles are accellerated toward the anode, and may be collected there if the charge attained is large enough. An expression for the velocity of the particle at any instant of time may be derived from two basic formulas. The motion of a particle in a viscous medium is described by Stokes' Law, which for a spherical body is

$$F = 6\pi n V_o R \tag{6}$$

where F is the force on the particle in dynes, n is the viscosity of the medium in poise, V_o is the terminal velocity of the particle in cm/sec, and R is the particle radius in cm. The electrostatic force on the particle is given by

$$F = Q e E \tag{7}$$

where Q is the particle charge in electrons, E is the field strength, and e is the charge on the electron. Eq (7) may be expresses as

$$F = 1.602 \times 10^{-12} Q E \tag{8}$$

where F is now the force in dynes, Q is the particle charge in electrons, and E is the field strength in volts/cm. Substituting Eq (8) into Eq (6) for air at 75°F and 1 atm on obtains

$$V = 4.73 \times 10^{-10} \frac{QE}{R} \tag{9}$$

This is true if it is assumed that terminal velocity is achieved instantaneously upon interaction of the force with the particle. While this assumption is not true, the time for the particle to achieve terminal velocity is small for the magnitude of the forces and particle radii under consideration.

It has been found that when the particle size is close to the mean free path of the molecules in the medium a correction must be added to Stokes' Law. This correction, known as the Cunningham correction to Stokes' Law is commonly used in the form of (Ref 3:310):

$$CUN = 1 + \frac{\lambda}{R} \left(A + Be^{-\frac{CR}{\lambda}}\right) \tag{10}$$

where λ is the mean free path of the medium in cm, and A, B, and C are constants given as 1.23, 0.41, and 0.88 respectively. At 20° C and 1 atm the mean free path of air molecules is reported by Davies as 9.42×10^{-6} cm (Ref 5:46). Substitution of these values into Eq (10) yields

$$CUN = 1 + \frac{9.42 \times 10^{-6}}{R}(1.23 + 0.41e^{-0.934 \times 10^{+5R}}) \quad (11)$$

The drift velocity in the ionization section is therefore:

$$V = (V_o)(CUN) \quad (12)$$

where V is the drift velocity in cm/sec. Substituting Eq (12) into Eq (9) one obtains for the drift velocity of the particle at any charge Q :

$$V = 4.73 \times 10^{-10} \frac{(Q)(E)(CUN)}{R} \quad (13)$$

Since the charge Q changes as the particle passes thru the ionization section Eq (13) may be more clearly expressed as:

$$V(I) = 4.73 \times 10^{-10} \frac{Q(I)\ E\ CUN(J)}{R(J)} \quad (14)$$

where V(I) is the drift velocity of the particle at any instant of time (I) in cm/sec, Q(I) is the charge achieved by the particle at that instant of time in electrons, CUN(J) is the Cunningham correction to Stokes' Law for a particle of size group J, and R(J) is the radius of a particle of size group J in cm.

By simply adding up the increment of distance traveled toward the anode by an aerosol with changing velocity one may obtain the fraction collected in the charging section by

$$FCC = \frac{DAC}{SEPC} \quad (15)$$

where DAC is the total distance traveled toward the anode in cm, and SEPC is the plate to wire separation distance in cm. It must be remembered that the fraction collected in the ionization section can never be greater than 1.0 and therefore Eq (16) is valid only for FCC greater than or equal to zero and less than or equal to 1.0.

Collection Section

Although a fraction of the aerosols may be collected in the ionization section, the collection section serves as the main mechanism for collection in the precipitation process. Since all of the particles have already traveled a certain distance, DAC, toward the anode in the ionization section, this must be considered in the calculation of the fraction collected in the collection section. The electric theory involved in the collection process is straightforward and elementary if certain assumptions are made. The assumptions (concerning turbulent flow and re-entrainment) will be presented during the discussion on efficiency and sensitivity.

Stokes' Law Terminal Velocity. Since no charging takes place in the collection section, the charge carried by a particle is constant and the expression for drift velocity takes on a different form than that of Eq (13). Stokes' Law however, holds during the collection process and was given by Eq (6) as:

$$F = 6\pi n V_o R \qquad (6)$$

where F is the force on the particle in dynes, n is the viscosity of the medium in poise, V_o is the terminal velocity of the particle in

cm/sec, and R is the particle radius in cm. Also, the electrostatic force on the particle is

$$F = 1.602 \times 10^{-12} QQ(ECOL) \tag{16}$$

where F is again the force in dynes, QQ is now the total charge the particle achieved while it was in the ionization section in electrons, and ECOL is the field strength between the collector plates in volts/cm. The field strength is linear in the collection process of a parallel plate precipitator and may be simply calculated by:

$$ECOL = \frac{V}{d} \tag{17}$$

where ECOL is the field strength between the collector plates in volts/cm, V is the applied potential between the plates in volts, and d is the distance between the plates in cm. Substituting Eq (16) into Eq (6) and solving for Vo in air at 75°F and 1 atm one obtains

$$Vo = 4.73 \times 10^{-10} \frac{(QQ)(ECOL)}{R} \tag{18}$$

Eq (18) differs from Eq (9) only in that the charge is not constant, and the electric field is that of the collection section. The assumption necessary for the derivation of Eq (9) is also made for Eq (18).

Cunningham Correction to Stokes' Law. Since the same particles that passed thru the ionization must be considered in the collection section, the Cunningham correction to Stokes' Law must again be applied. Eq (11) gives this correction for air at 20°C and 1 atm as:

$$CUN = 1 + \frac{9.42 \times 10^{-6}}{R}(1.23 + 0.41e^{-0.934 \times 10^{5R}}) \tag{11}$$

where R is the particle radius in cm . The corrected drift velocity becomes:

$$VD = Vo(CUN) \tag{19}$$

where VD is the drift velocity in cm/sec, Vo is the terminal velocity according to Stokes' Law in cm/sec, and CUN is the Cunningham correction to Stokes' Law.

Fraction Collected in the Collection Section. A certain fraction of the particles that are not collected in the ionization section are collected in the collection section. This fraction depends on the parameters that affect the efficiency of the collection section. The distance a particle travels toward the anode in the collection section is given by

$$DA = \frac{(VD)(DL)}{(VLCL)} \tag{20}$$

where DA is the distance traveled toward the anode by the particle in the collection section in cm, VD is the drift velocity in cm/sec, DL is the length of the collection plates in cm, and VLCL is the velocity of air flow in the collection section in cm/sec. Therefore the fraction collected in the collection section may be expressed by

$$FC = \frac{DA}{(SEP - DAC)} \tag{21}$$

where FC is the fraction of aerosols that leave the ionization section that are collected in the collection section, DA is the distance these aerosols travel toward the anode in the collection section in cm, SEP

is the distance between the collector plates in cm, and DAC is the distance traveled toward the anode by the particles while they were in the ionization section in cm. Since the fraction collected can never be greater than unity, the problem solution must set FC equal to 1.0 if the distance traveled toward the anode is such that the computed value of the fraction collected is greater than 1.0.

Total Fraction Collected. Although the fractions collected in the ionization and collection sections are interesting quantities, the most important quantity used to calculate the total amount of particles collected is the total fraction collected. The total fraction of particles collected during the entire precipitation process is equal to the fraction collected in the ionization section, plus the fraction collected in the collection section multiplied by the fraction leaving the ionization section, or

$$FRTO = FCC + (1 - FCC)\, FC \tag{22}$$

where FRTO is the total fraction collected, FCC is the fraction collected in the ionization section, FC is the fraction collected in the collection section, and the quantity (1 - FCC) is the fraction leaving the ionization section.

Sensitivity and Efficiency. The precipitator sensitivity as discussed in Chapter I, is probably the most important measure of success of the design itself. Higher sensitivity however, usually results in lower efficiency, and the material and equipment available may necessitate a compromise between the two. Sensitivity was defined by Eq (1) as

$$SEN = (EFF)(VOL) \tag{1}$$

where SEN is the sensitivity of the machine in m^3/min, EFF is the efficiency of the precipitator, and VOL is the volume flow of air thru the precipitator in m^3/min. The efficiency of the precipitator for a particular size group particle may be expressed as

$$EFF = (FR)(FRTO) \tag{23}$$

where FR is the mass fraction of a particular size group from Table I, and FRTO is the total fraction collected of that size group. Substitution of Eq (23) into Eq (1) yields:

$$SEN = (FR)(FRTO)(VOL) \tag{24}$$

where SEN is the sensitivity of the precipitator for a particular size group in m^3/min. The summation of sensitivities for all size groups will give the total sensitivity of the precipitator.

The above calculations are valid if two assumptions are made. First, it is assumed that the flow is laminar throughout the entire precipitation process. This will not be true for certain cases, but the assumption is conservative for efficiencies above 50%, and leads to a maximum deviation of 10% from the true efficiency where the collector length is one fifth that necessary for complete removal of all the particles, a length corresponding to an efficiency of around 20% (Ref 8:72) In view of the above assumption, it is perhaps worthwhile to know at what velocity the transition from laminar to turbulant flow takes place. The flow in a parallel plate collection section can be assumed turbulant if (Ref 8:85):

$$\frac{VH}{\nu} \geq 8500 \tag{25}$$

20

where V is the flow velocity in ft/sec, H is the distance between plates in ft, and ν is the kinematic viscosity of the medium in ft^2/sec. For air at $60^\circ F$, ν is about 0.59 ft^2/hr (Ref 8:86), and therefore the transition velocity for plates 2 cm apart is

$$V(cm/sec) = (8500)(0.59 ft^2/hr)(hr/3600 sec)(930 cm^2/ft^2)(1/2 cm)$$
$$= 650 \text{ cm/sec}$$

Therefore at flow velocities above 650 cm/sec the flow can be considered turbulent for a precipitator whose plates are spaced 2 cm apart.

The second assumption made is that all particles striking the collector plates become attached and are not later dislodged by the air flow or other particles being collected. This assumption is not true and theory pertaining to the dislodgement and re-entrainment of particles is both difficult and incomplete. However Rose and Wood (Ref 8:73) show that the maximum deviation from the efficiency calculated from simple theory is 20%. This maximum deviation occurs where the simple theory, neglecting re-entrainment predicts the efficiency to be 100%. This deviation decreases as the efficiency decreases. It should be mentioned however, that experience has shown that the experimental efficiency is always less than the theoretical efficiency (Ref 8:84). It should also be mentioned that the velocity range that the precipitator is operating in will influence the maximum deviation.

Summary

Although the theory presented for the purposes of this thesis is straightforward and simple, it must be remembered that several necessary

simplifying assumptions were made. The theory of electrostatic precipitation is not new, but it is incomplete. Until better, more complete theory, is available, the procedure presented is believed to be the most complete to date. The correct form of the efficiency equation is one of the outstanding problems of precipitator theory today (Ref 8:152). Although the results obtained using the theory presented will not be exactly correct, it is believed that its use in the understanding and design of electrostatic precipitators is invaluable. This will be especially true in the optimization study of an electrostatic precipitator, where better theory is probably not required because only the optimum parameters are sought. More complete theory would give more accurate results, but would probably not help to determine the optimum operating parameters much more accurately. This is also true in design studies since they are primarily based on optimization.

The theory presented in this chapter requires a detailed experimental verification. Only until this is accomplished will the accuracy of the theory presented be in question.

III. Analysis of EARC I

The purpose of this chapter is to analyze an actual design of the two stage electrostatic precipitator named EARC I. The analysis will show the charge attained by each group, the fraction of each group that is collected in both the charging and collecting sections, as well as the sensitivity and efficiency of the machine. This chapter will also demonstrate the pronounced effect of varying the flow velocity, charging voltage, and corona current parameters. As a result of these calculations certain conclusions will become obvious. The conclusions will be of significant value in the next chapter which deals with the optimization of an electrostatic precipitator.

Design

The design specifications of EARC I are illustrated schmatically in Fig. 1. As can be seen from Fig. 1, EARC I is a two stage parallel plate precipitator with a rectangular cross section. Ionization occurs by negative corona discharge since the wire cathodes are maintained at -21.7 Kv. The negativily charged aerosols are collected at the grounded anodes of both the charging and collecting sections. The plexiglass insulators between the cathodes of the ionization and collection section eliminates leakage or corona discharge which might occur from the potential difference of 3.7 Kv at that location.

The high voltage supply is a NJE Corporation product, model H30-35, with a rating of 30 Kv and 35 ma. Outside air is drawn thru the precipitator by means of an ILG Ventilating Company (model BU 1350) centrifugal fan rated at 1.5 HP and a free flow of 3200 cfm.

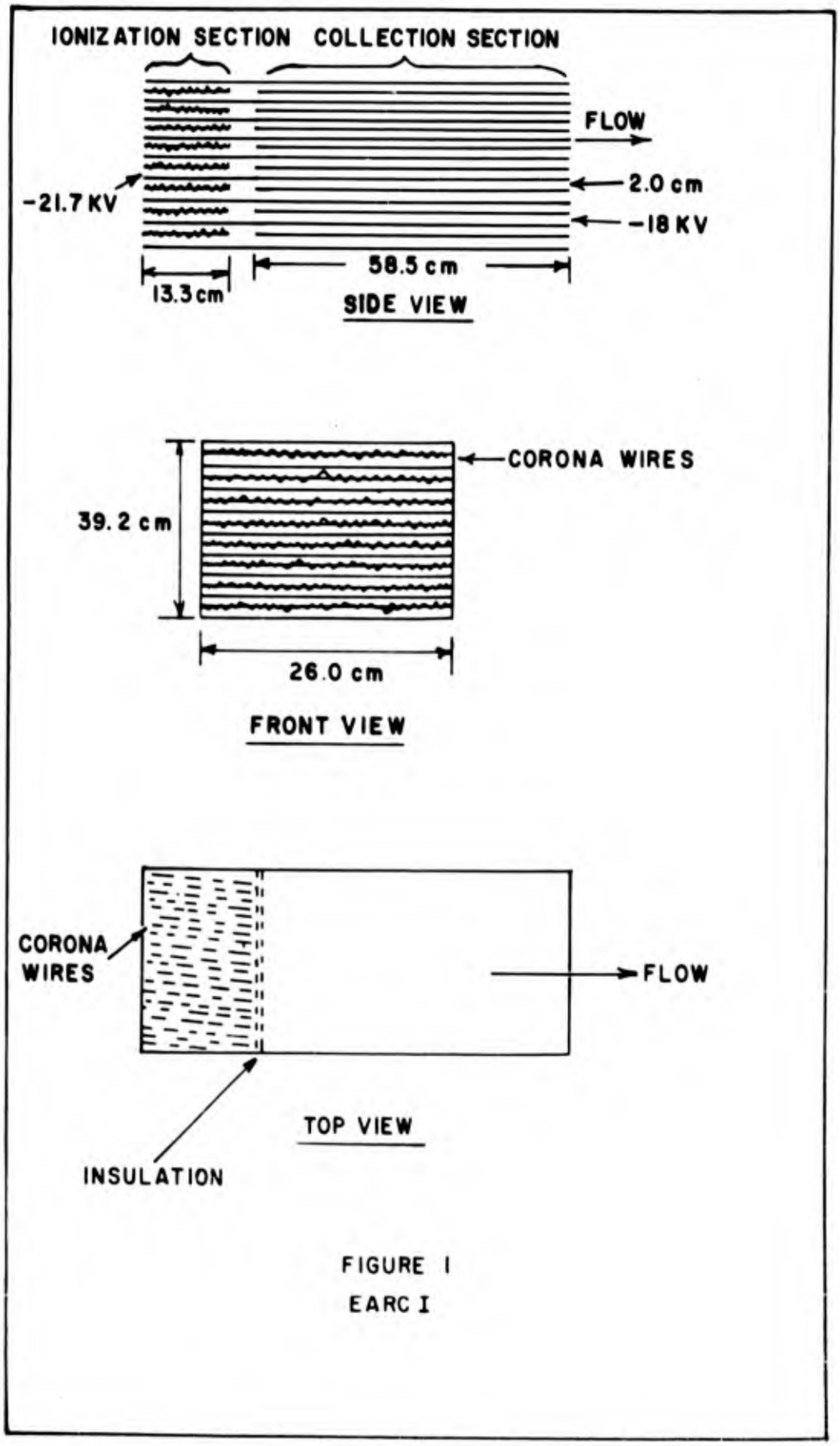

FIGURE I
EARC I

Charging Section. As shown in Fig. 1 the charging section consists of eight aluminum frames wound with 5 mil Tungsten wire. The grounded aluminum plates are part of the collecting plates extending forward from the collection section. These plates are spaced 2.0 cm apart and are held in position by slots cut lengthwise along the inside of the plexiglass outer shell.

Collection Section. The plates that make up the collection section are polished aluminum and are also placed 2.0 cm apart. The potential placed across the collection plates is 18 Kv, a value only slightly lower than that placed across the corona wire-plate combination in the ionization section.

Operating Parameters. The computer program (Appendix A) is designed to accept eleven variable parameters which of course are, in this case fixed by design and operating conditions. Input data (R(J), FR(J)) is taken from Table I, and values for the Cunningham correction factor are calculated from Eq (11). Values of accept data inserted into the computer program for the EARC I analysis are as follows:

E - 10850	volts/cm	SEP - 2.0	cm
CUR - .00125	amps/wire set	VLCL - 964	cm/sec
VL - 964	cm/sec	DL - 58.5	cm
SEPC - 2.0	cm	FRAR - 832	cm
AREA - 346	cm	ECOL - 9000	volts/cm
DCH - 13.3	cm		

where E is the electric field in the ionization section, CUR is the corona current in the ionization section, VL is the flow velocity in

the ionization section, SEPC is the plate to wire separation distance, AREA is area of the corona wire cathode, DCH is the charging length, SEP is the plate separation distance in the collection section, VLCL is the flow velocity in the collection section, DL is the collection plate length, FRAR is the frontal area of the precipitator (frontal area of plates subtracted from total frontal area), and ECOL is the electric field between the collection plates. It should be noted at this point that the electric field E, is assumed to be linear, and this assumption should not lead to great error (Ref 6:96).

Results

EARC I normally operates at the operating conditions presented. It is possible however, to operate at lower values of voltage, current, and flow velocity. This presentation therefore not only indicates the results for the normal operation of EARC I, but also shows what results might be expected if EARC I were operating at lower charging voltage and currents and higher velocity.

The computer program is designed to print out values of charge achieved, fraction of particles collected in the ionization section, fraction of particles collected in the collection section, and total fraction of particles collected for each size group. The program is also designed to print out sensitivity, efficiency, volume flow, and time spent in the charging section.

Charge Achieved. The electrons achieved by both bombardment and diffusion charging by each particle group are presented in Table II. Figs. 5 and 6 are plots of charge (Q(I)) vs time spent in the ionization section (T), for groups 1 and 12 respectively.

Fractions Collected. The charged aerosols may be collected either in the charging section or the collection section depending on their size. The fraction of EARC I particles that are collected in the charging section (FCC) is illustrated by means of a size group histogram in Fig. 2. A fraction of the particles that escape collection in the charging section are collected in the collection section. This fraction is the fraction collected in the collection section (FC) and is also shown by means of a size group histogram in Fig. 3. The total fraction collected (FRTO) is a measure of the efficiency and is a combination of the fraction collected in the charging section and the fraction collected in the collection section. This total fraction collected is given by Eq (22) as

$$FRTO = FCC + (1 - FCC)FC \tag{22}$$

The total fraction collected for each size group is presented in Fig. 4.

Sensitivity and Efficiency. Sensitivity is defined by Eq (24) as

$$SEN = (FR)(FRTO)(VOL) \tag{24}$$

where FR is the mass fraction for the size group under consideration from Table I, FRTO is the total fraction collected and VOL is the volume flow of air. Since EARC I is operating at a volume flow of 48.07 m^3/min the summation of sensitivities for all twelve size groups yield a total sensitivity of 44.49 m^3/min. The efficiency of EARC I is calculated to be 92.55 %.

Variable Flow Effects. Changing the flow rate may have an appreciable effect on the value of efficiency and sensitivity. Flow rates

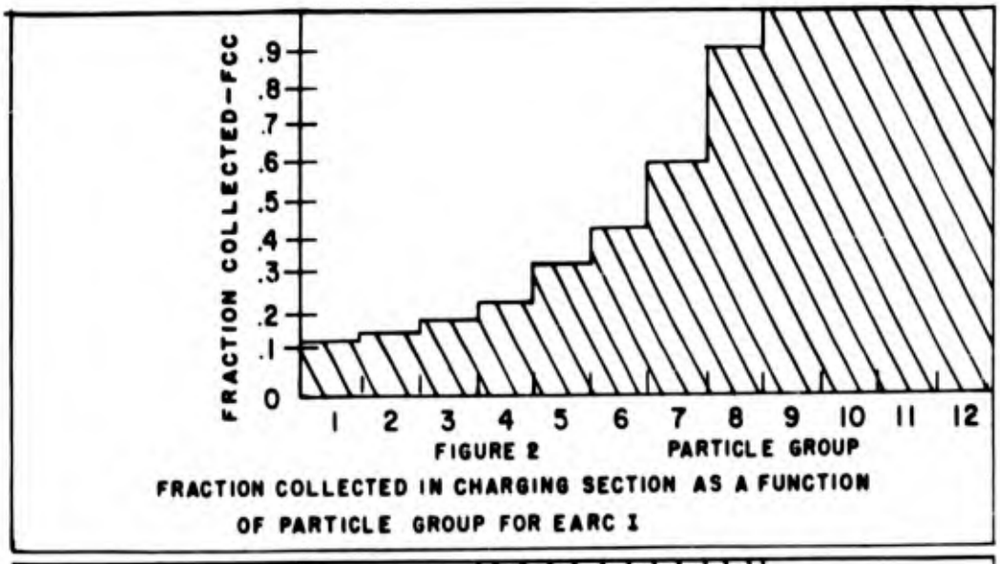

FIGURE 2

FRACTION COLLECTED IN CHARGING SECTION AS A FUNCTION OF PARTICLE GROUP FOR EARC I

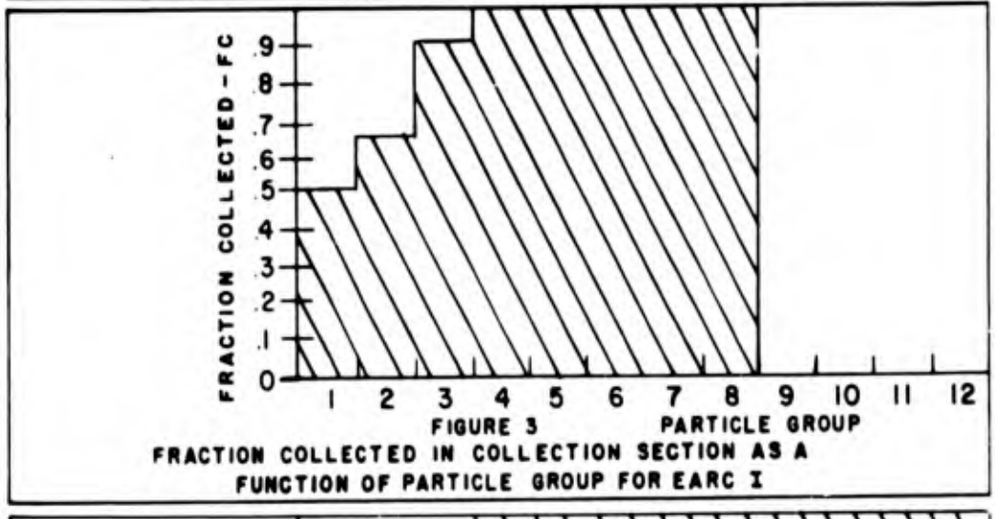

FIGURE 3

FRACTION COLLECTED IN COLLECTION SECTION AS A FUNCTION OF PARTICLE GROUP FOR EARC I

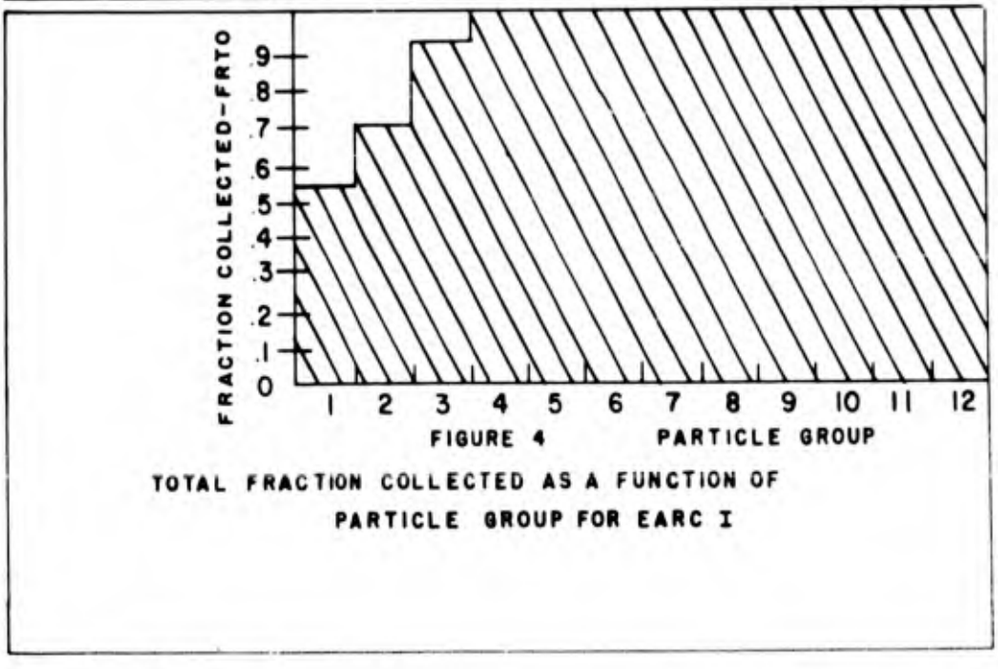

FIGURE 4

TOTAL FRACTION COLLECTED AS A FUNCTION OF PARTICLE GROUP FOR EARC I

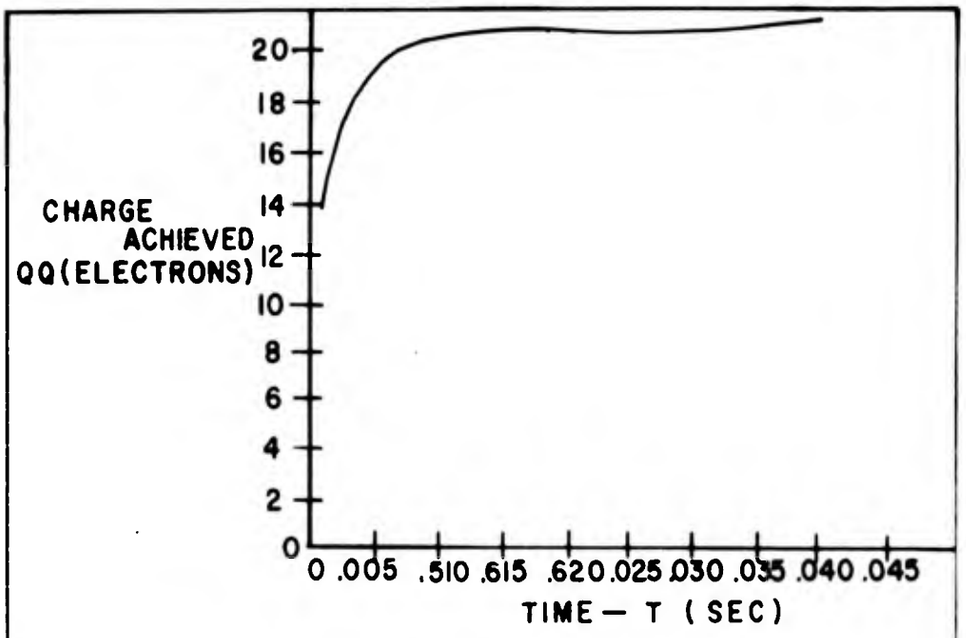

FIGURE 5

CHARGE ACHIEVED AS A FUNCTION OF TIME SPENT IN CHARGING SECTION BY A GROUP 1 (.125u) PARTICLE IN EARC 1

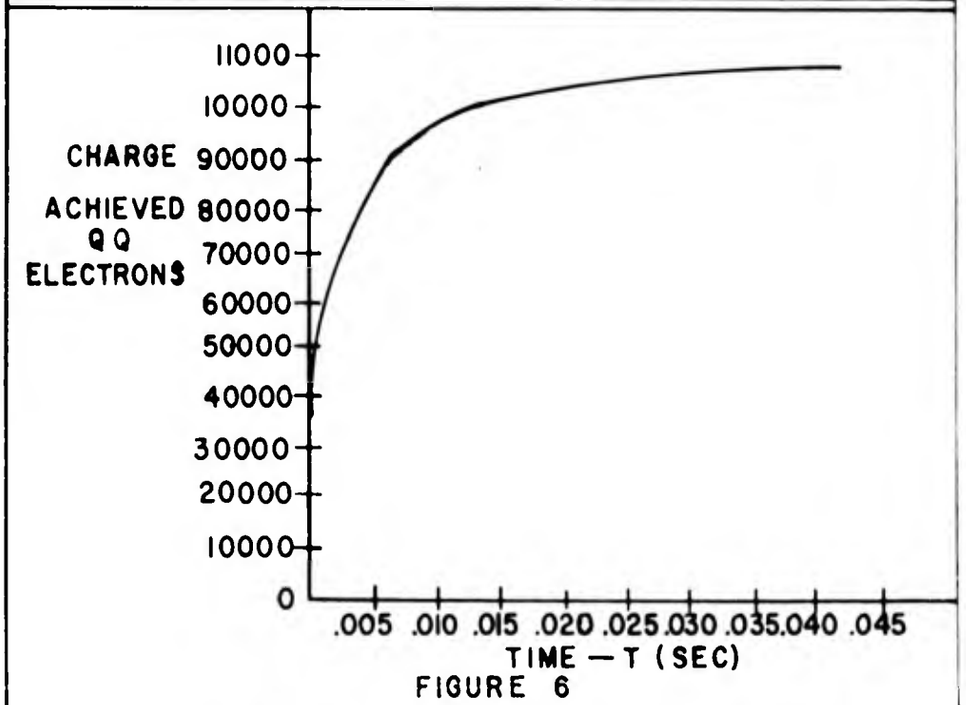

FIGURE 6

CHARGE ACHIEVED AS A FUNCTION OF TIME SPENT IN CHARGING SECTION BY A GROUP 12 (8.5 u) PARTICLE IN EARC 1

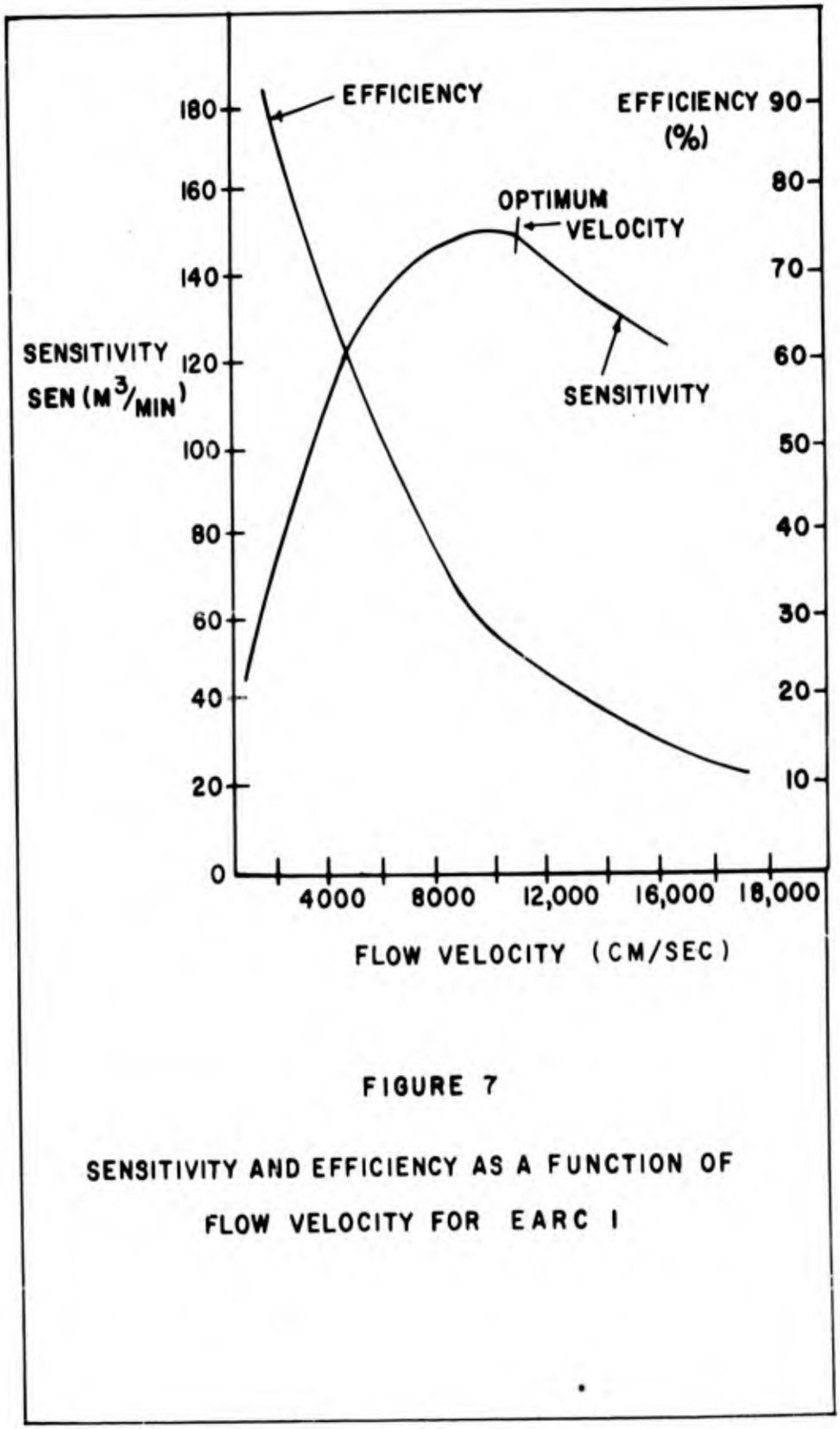

FIGURE 7

SENSITIVITY AND EFFICIENCY AS A FUNCTION OF FLOW VELOCITY FOR EARC I

Table II
Computed Results for EARC I

Group	Avg. Radius (u)	Particle Charge QQ(Elec)	Fraction Col Chrg Sect FCC	Fraction Col Collection Sect FC	Total Fraction Collected FRTO
1	.125	21	.11	.51	.56
2	.200	56	.13	.67	.67
3	.300	126	.18	.91	.91
4	.425	253	.23	1.00	1.00
5	.600	504	.31	1.00	1.00
6	.850	1012	.42	1.00	1.00
7	1.250	2190	.59	1.00	1.00
8	2.000	5607	.92	1.00	1.00
9	3.000	12616	1.00	0.00	1.00
10	4.250	25.321	1.00	0.00	1.00
11	6.000	50.466	1.00	0.00	1.00
12	8.500	101284	1.00	0.00	1.00

Volume Flow	Sensitivity	Efficiency
48.07 m^3/min	44.49 m^3/min	92.55%

Ion Density	Corona Current	Bombardment Sat Chg
1.17×10^9 ions/cm^3	1.25×10^{-3} amps	93%

Note: All charges are rounded off to the next lower electron charge since an aerosol cannot have a partial electron charge. The flow rate of 964 cm/sec corresponds to a charging time of .0137 sec.

Table III •
Flow Rate Effects on Sensitivity and Efficiency for EARC I

Velocity VL(cm/sec)	Sensitivity SEN(m^3/min)	Efficiency EFF (%)
964	44.49	92.55
2000	75.37	75.55
5000	125.86	50.46
9000	148.19	33.01
11000	148.27	27.02
12000	144.35	24.11
13000	140.06	21.60
14000	136.12	19.49
16000	129.18	16.18
19000	120.60	12.72

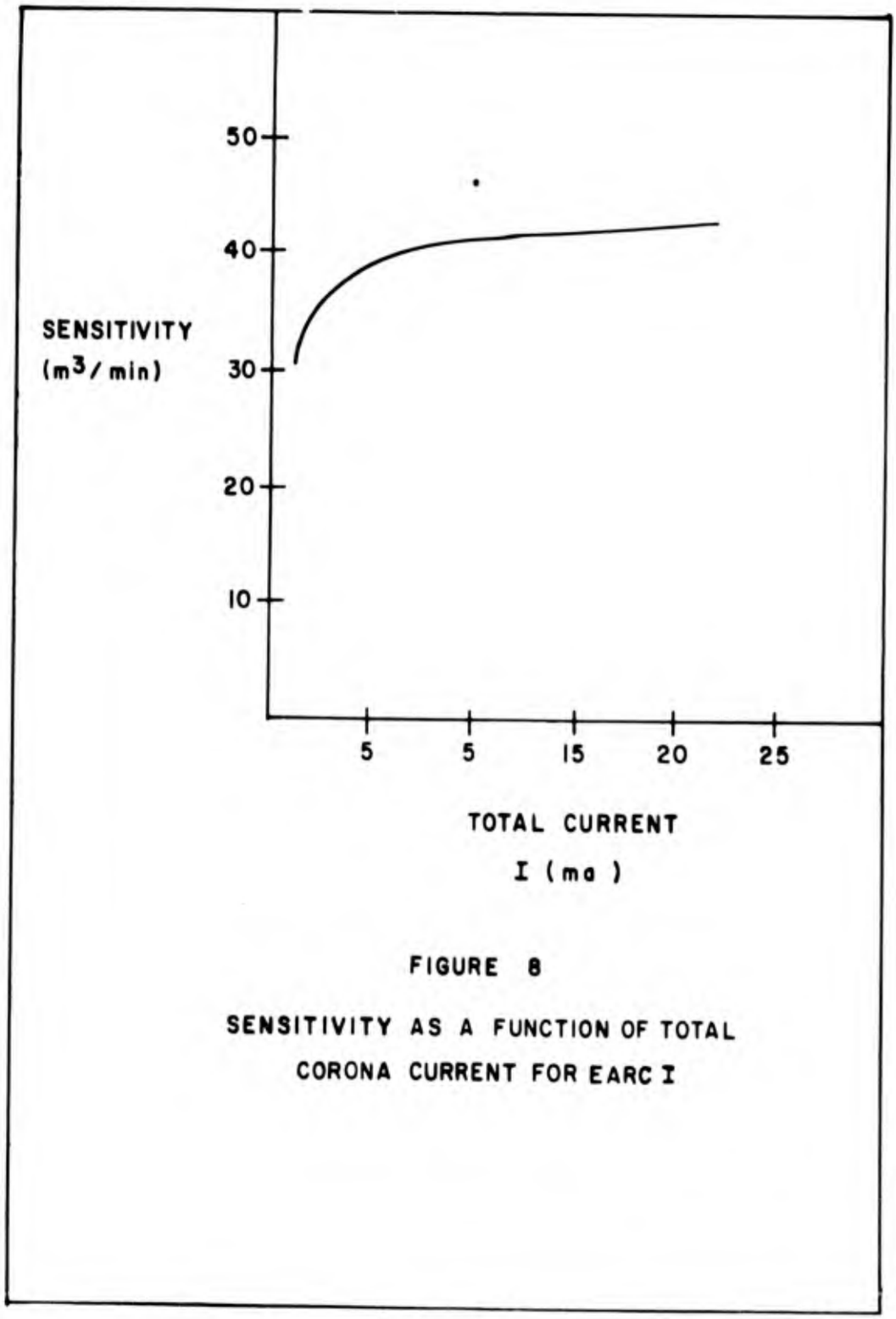

FIGURE 8

SENSITIVITY AS A FUNCTION OF TOTAL CORONA CURRENT FOR EARC I

Table IV
Effects of Corona Current on Sensitivity
and Efficiency for EARC I

Total Current I (ma)	Electric Field E(Volt/cm)	Sensitivity SEN(m^3/min)	Efficiency EFF(%)
.6	7250	30.07	62.54
1.4	7750	35.19	73.22
2.9	8200	38.43	79.94
4.2	8500	39.86	82.92
6.2	8800	40.94	85.15
8.0	9150	41.71	86.80
11.0	9450	42.58	88.56
13.2	9800	43.17	89.78
16.3	10150	43.66	90.82
20.0	10850	44.49	92.55

for EARC I were varied from the actual rate of 964 cm/sec to 19000 cm/sec. The effects of theoretically changing the flow rate for EARC I are presented in Table III and graphically in Fig. 7.

Voltage and Current Effects. The operator of EARC I has a wide choice of voltage and current operating conditions in the charging section. Table IV gives the values of voltage and current that will result in precipitation (Ref 1:Chapter III). Sparking may take place at high voltages and currents, especially on days when there is a large amount of moisture in the air. It may be necessary therefore, to operate at a lower value of voltage and current in order to prevent excessive arcing. The sensitivity of EARC I as a function of corona current is presented graphically in Fig. 8.

Bombardment Saturation Charging. The fraction of saturation charge achieved by bombardment (FQQ) may be calculated by Eq (5) which is

$$FQQ = \frac{1}{1 + \frac{1}{(8.03 \times 10^{-7} G)(T)}} \tag{5}$$

where FQQ is the fraction of saturation charge achieved, G is the ion density in ions/cm^3, and T is the time that the particle is in the charging section in sec.

Using the parameters for EARC I from page 25, the value of G is calculated to be 1.172×10^9 ions/cm^3 and T is 0.0137 sec. These values result in a value of FQQ equal to .93. A quick visual validation of this figure can easily be achieved by comparing the value of charge Q at T = 0.0137 sec and at a much larger time on Fig. 6.

Discussion of Results

The preceeding results bring to light many interesting theoretical facts from which one may draw reasonable conclusions. By using the electronic digetal computer as a tool in solving the differential equation and the problem in general, a great deal of informative results was compiled.

It is easy to see that EARC I has a very high rate (m^3/min) of dust collection compared to the best filter systems available today. That is to say that EARC I has a collection rate of 44.49 m^3/min as compared to the Staplex high volume air sampler (model TF1A with filter type TFA-41) which has a collection rate of approximately 1 m^3/min. Therefore it would appear that EARC I would require a sampling time 1/45 of that of the Staplex filter to collect the same amount of dust. This fact alone is enough to inspire one to look further into the possibility of using the electrostatic precipitator as a means of sampling the air for radioactive content.

Another interesting result of the analysis is the charge achieved by each size group and the time required to achieve this charge. As might be intuitively expected, the charge achieved by each particle is dependent upon its size if all other parameters are held constant. The number of electrons each group of particles achieve varies from 21 electrons for the group 1 particles to 101,284 electrons for the particles in the twelfth group. The charge achieved by each group increases with group size. The change in charge Δq divided by the change in particle radius Δr between the first and second group particles is 467 electrons/u, and between the eleventh and twelfth group

is 20,150 electrons/u, showing the relationship of particle area to charge achieved (Ref 4:36). Figs. 5 and 6 show the charge achieved as a function of time spent by a particle in the charging section for groups 1 and 12 respectively. As can be seen from these figures the particles achieve almost all of their charge within the first few units of time. The fraction of saturation charge (bombardment) achieved by bombardment charging for EARC I particles is .93. This value corresponds to a charging time of 0.0137 sec.

Figure 8 shows the value of sensitivity as a function of corona current at all possible voltage and current operating conditions. It is clear from Fig. 8 that an increase in current always results in an increase in sensitivity. The most interesting results from Fig. 8 is the fact that an increase in current at low values of currents result in a greater increase in sensitivity than the same increase in current at currents near the sparkover value. One might conclude therefore, that if certain operating conditions (atmospheric moisture) near the sparkover value of current result in frequent sparkovers and consequent machine shutdown, EARC I may be operated at a slightly lower current and the sensitivity will not be lowered prohibitively.

Many interesting events take place in the collection process. A significant amount of the larger size particles are collected in the ionization section before the particles have even entered the collection section. The theoretical results show that all of the particles in the four largest size groups are collected in this manner. Experiments with EARC I (Ref 1:Chapter III) show a large amount of dust

being collected on the plates in the ionization section. This of course agrees well with the theoretical results.

A measurable amount of all size groups considered are collected. Results show that 56% of the smallest size group are eventually collected. One may conclude that for EARC I the smallest size group is the hardest to collect. This is true because the smallest size group particles achieve a relatively small amount of charge compared to the amount of charge achieved by the large size particles, and the ratio of charge achieved to the particle radius for the small size particles overrides the increase in the Cunningham correction factor in the drift velocity equation (Eq (18)). The result is a lower drift velocity for the smaller size particles and therefore a lower fraction of the small size particles are collected.

One of the most important results of the analysis of EARC I is the change occuring in sensitivity as the flow velocity is varied. The sensitivity increases to a velocity of 11000 cm/sec and then decreases in what appears to be a linear fashion. Fig. 7 shows the sensitivity peak to be at 11000 cm/sec and this would correspond to the velocity at which EARC I should operate to achieve maximum sensitivity. EARC I is operating at the low end of the curve and any increase in velocity up to 11000 cm/sec would theoretically result in an increase in sensitivity. At this point one should mention that the probability of losing collected particles by the high velocity air or re-entrainment has not been considered in this analysis. It may be found experimentally, that high velocities may dislodge the already collected particles.

As can easily be seen, EARC I is operating at a very high efficiency. An efficiency of 92.55% can be considered quite high but as has already been stated, the efficiency does not tell the whole story. The efficiency of EARC I decreases with increasing flow velocity as can be seen from Fig. 7. This curve resembles an exponential function of the form of

$$EFF = 100e^{(A)(VL)} \% \tag{26}$$

where A is a constant for a particluar model precipitator operating at fixed parameters except for a changing flow velocity. Equation (26) is a good representation of the efficiency curve except for the low end of the velocity spectrum. It may be that an end correction term is necessary at low velocity and that the value of the constant A may be a measure of the performance of different precipitators or a method of comparing the relative merit of each. The velocity seems to be the easiest parameter to vary once the precipitator is designed and in operation. The value of A for EARC I is -9.3×10^{-5} sec/cm. Although EARC I is operating at the high end of the efficiency range, an increase in velocity to increase sensitivity would decrease the efficiency. It should be noted that theoretically, an efficiency of 100% would correspond to a sensitivity equal to zero, and an efficiency of zero would also correspond to a sensitivity of zero.

To conclude the analysis of EARC I, it can be stated that the machine is capable of producing good results under its present operating conditions. The sensitivity of EARC I can theoretically be

increased fourfold by simply increasing the flow velocity. This may however, require a fan that is prohibitive in cost or size.

IV. Precipitator Optimization

General

The purpose of this chapter is twofold. The primary purpose of this chapter is to study the effects of varying the parameters involved in the electrostatic precipitation process, and attempt to optimize a two-stage parallel-plate precipitator (EARC I). The secondary purpose is to present a better understanding of the parameters and their effects in order to give the designers of future precipitators an idea of what can be achieved in the way of results from the use of electrostatic precipitators for radioactive air sampling. Each precipitator stage will be presented seperately after which the combination of the two stages will lead to the optimum design and certain definite conclusions.

The two stage electrostatic precipitator has many parameters that may be varied as was clearly demonstrated in Chapter III. There are eleven parameters that may be varied, any one of which will result in a change in sensitivity. A number of the parameters are interdependent, and a change in one parameter will result in a change in another. The scope of this thesis does not permit a detailed study of the effects of each parameter. Since the theory of electrostatic precipitation is not complete at this time, some of the parameters will be held constant. The parameters involved in each stage will be studied seperately, the constant ones being outlined under the specification section for each stage.

Ionization Section

The first stage of the precipitation process is the ionization section. The main purpose of the ionization section is to supply or make available free ions for attachment to the incoming aerosols. A number of parameters affect the charging rate of the aerosols and (at a fixed power setting) may be classified as mainly time, distance and velocity. It will be shown however, that the power supply determines the charging distance and therefore sets the time for charging with a given velocity. All of the parameters that effect the collection section will be held fixed while the ionization section is optimized.

Specifications. The most important piece of support equipment to be considered in the design of an electrostatic precipitator is the high voltage power supply. For the purpose of this chapter it is assumed that the power supply available is a NJE Corporation model HHO 50-50, capable of producing 50 kv with a maximum continuous current of 50 ma. The air flow supply is assumed to be unlimited but the frontal area of the precipitator (allowing for individual plate frontal area) is set at 832 cm^2. The width of the precipitator is fixed at 26 cm and the height at 39.2 cm. The charging section is assumed to contain sixteen sets of plates and wires of variable length. During the optimization analysis of the ionization section, the collection section parameters are set constant at sixteen sets of plates 58.5 cm long, 2 cm apart with an electric field of 9000 volts/cm present between each set of collection plates.

Velocity Effects. As was demonstrated in Chapter III, a change in flow velocity will result in a change in sensitivity. A particular

velocity will produce an optimum sensitivity if all of the other parameters are held constant. Since the sensitivity is a function of velocity, the air flow will often be varied at the same time the other parameters are varied. If all parameters are held constant, except velocity, a curve of the form of Fig. 9 will result. The peak of the curve, or the point where the sensitivity is greatest, yields the desired operating velocity. With the aid of Eq (1) the velocity vs sensitivity curve is divided into three sections each of which will now be analyzed separately. In the first section, during the sensitivity rise, the precipitator has a high efficiency but a low velocity. The sensitivity increases as the velocity is increased because the volume flow of air is increasing faster than the efficiency decreases. In the second section of the curve the efficiency decreases at about the same rate as the velocity increases and the curve approaches the peak. At the peak, the efficiency is decreasing at exactly the same rate as the velocity is increasing and the optimum velocity is achieved. Section III starts immediately after the peak. In this section of the curve the efficiency is decreasing faster than the velocity is increasing, and therefore the sensitivity decreases.

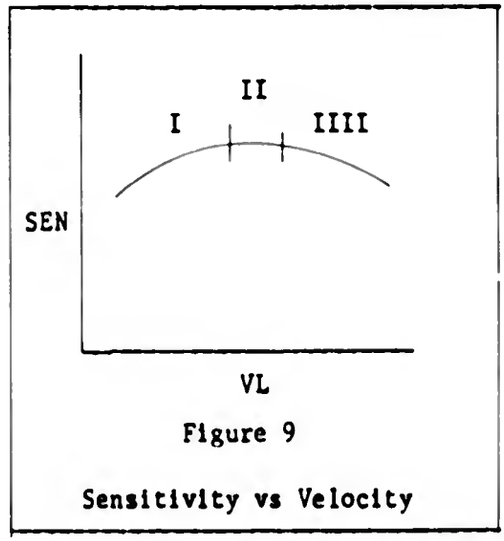

Figure 9

Sensitivity vs Velocity

Power Effects. Once a power supply is selected the precipitator may operate at any voltage and current from the corona starting voltage

up to a value just below the voltage that will result in sparkover. Table IV gives the experimental values for voltage and current obtained for EARC I. Fig. 8 shows how the sensitivity varies with corona current for EARC I. This figure clearly shows that the sensitivity varies only slightly as the voltage and current is varied at a constant velocity of 964 cm/sec. If the velocity is varied along with the voltage and current, the results are quite interesting. Fig. 10 shows the results for three velocities. The first velocity is at 964 cm/sec (EARC I). The change in sensitivity is slight. An increase of 14.42 m^3/min results throughout the complete range of power values. The second curve is at EARC I's optimum velocity of 11000 cm/sec. The curve has almost approached a straight line with an increase of 138.63 m^3/min throughout the complete power range. The third curve shows the sensitivity variation for a high velocity (19000 cm/sec). This curve is also almost a straight line but at lower values of sensitivity. If curves for velocities between the values stated were plotted, they would rise from the low velocity until the optimum velocity is reached, then fall to the right of the optimum velocity curve and approach the 19000 cm/sec curve. As the velocity is increased past the 19000 cm/sec value it is reasonable to believe the curve would continue to fall until the sensitivity was zero for any velocity greater than that necessary to make the efficiency zero. It is interesting to note that for a value of I equal to about 3.0 ma, the sensitivity is about the same for any of the three velocities stated.

The foregoing results show that the operating power conditions are especially important at the optimum velocity, and if the precipitator

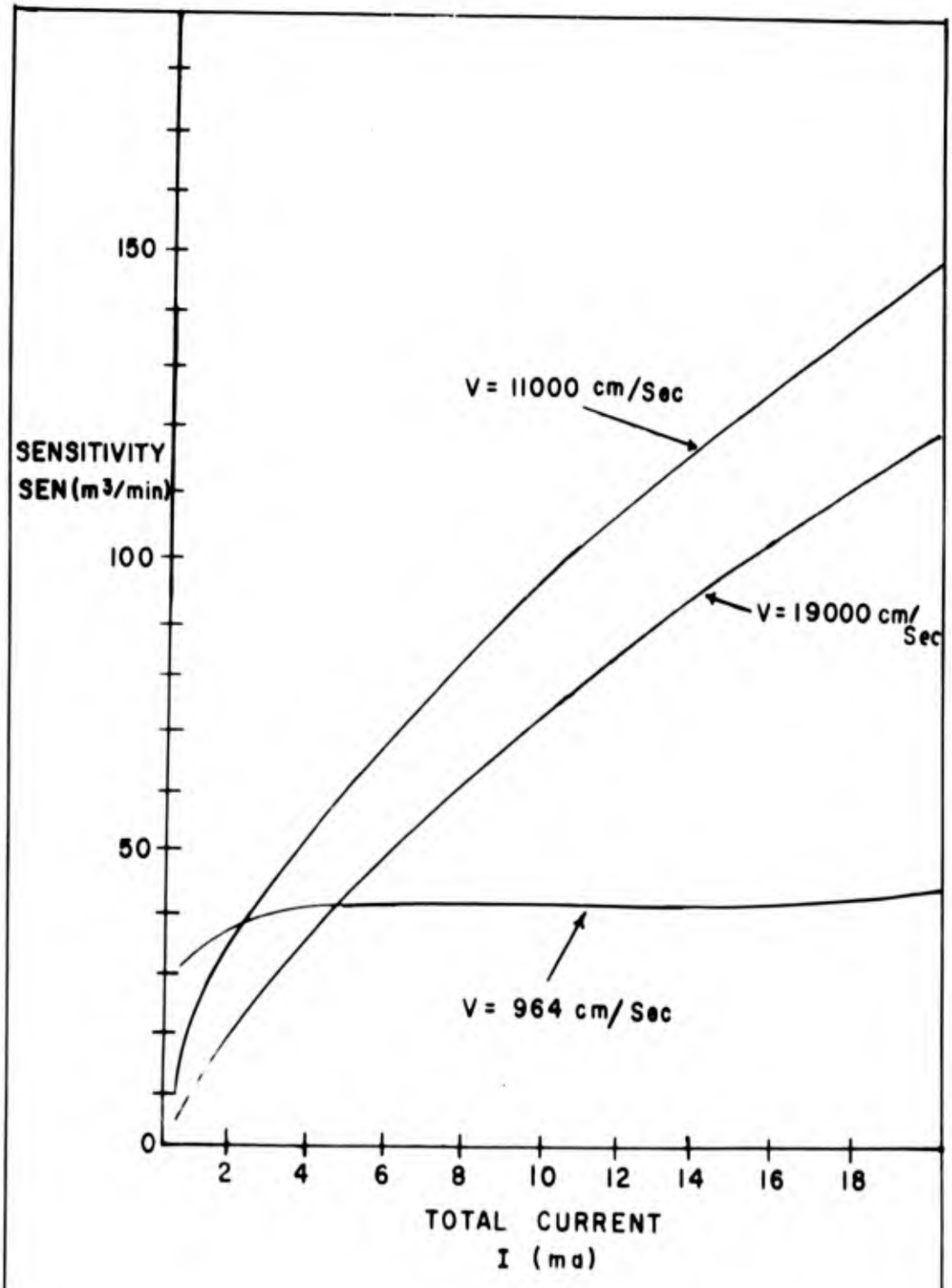

FIGURE 10

SENSITIVITY VS TOTAL CORONA CURRENT AT THREE VELOCITIES

is operated at a very low velocity the power conditions are not as critical. That is to say that although a high current and voltage is always desirable, the high values are especially critical when operating at the optimum velocity.

Charging Distance. It has been shown that a high corona current is always desirable. Once a precipitator is designed, the only way the current can be increased is to increase the applied voltage until just before sparkover occurs. However, the current (amps/set of plates and wires) may be increased during the design stage by increasing the charging length. Eq (3) gives

$$CUR = (Z)(L) \tag{3}$$

where Z is a constant dependent on wire size and material in amps/cm and L is the length of wire in cm. As the length of wire is increased, the current (amps/set) is also increased. If the number of charging sets are fixed at sixteen, the total current (I) may be given as

$$I = (CUR)(16) \tag{27}$$

because the maximun current permitted is determined by the power supply (50 ma), the maximum current permitted is 3.12×10^{-3} amps/set.

The value of the constant Z in Eq (3) may be determined for 5 mil tungsten wire by using the experimental results from EARC I. Since the charging cathode consists of 23 turns of wire spaced 1.13 cm apart, and the charging distance is 13.3 cm the length L is given by

$$L = 23(13.3^2 + 1.13^2)^{1/2}$$

$$= 307 \text{ cm}$$

and the value of CUR for EARC I is found experimentally to be 1.25×10^{-3} amps/set, the value of Z is therefore

$$Z = \frac{CUR}{L} \tag{28}$$
$$= \frac{1.25 \times 10^{-3} \text{amps/set}}{307 \text{ cm}}$$
$$= 4.07 \times 10^{-6} \text{ amps/cm}$$

The value of current for any length may be expressed as

$$CUR = 23(DCH^2 + 1.13^2)^{1/2}(Z) \tag{29}$$

where CUR is the current shared by the cathode anode set in amp, and DCH is the length of the charging section in cm.

The current density (amps/cm^2) may be assumed constant if care is taken to position the cathode wires properly. The current density for EARC I may be easily determined by dividing the current (amps/set) by the cathode area. The current density is given by

$$\frac{CUR}{AREA} = \frac{1.25 \times 10^{-3} \text{amp}}{346.0 \text{ cm}^2} \tag{30}$$
$$= 3.62 \times 10^{-5} \text{ amps/cm}^2$$

It should be noted that this value is assumed to be the maximum permissible because a higher value would probably result in sparkover. If the maximum permissible current, CUR, is set by the power supply at 3.12×10^{-3} amps, then the maximum charging distance may be found by either Eq (29) or Eq (30). Rearranging Eq (30), the maximum AREA is found by

$$\text{AREA max} = \frac{\text{CUR max}}{3.62 \times 10^{-6} \text{amps/cm}^2} \tag{30}$$

$$= \frac{3.12 \times 10^{-3}}{3.62 \times 10^{-6}}$$

$$= 837.2 \text{ cm}^2$$

if the AREA is also equal to the charging distance (DCH) multiplied by the precipitator width (26cm), the maximum charging distance permissable for a 50 ma power supply is therefore

$$\text{DCH(max)} = \frac{\text{AREA(max)}}{26.0} \tag{31}$$

$$= \frac{837.2 \text{ cm}^2}{26.0 \text{ cm}}$$

$$= 32.0 \text{ cm}$$

The end result is that the charging distance may not be longer then 32 cm if the total current is to remain below the 50 ma capability of the power supply.

It is interesting to note the effects that changing the charging distance has on the sensitivity and efficiency. Tables V and VI show these effects for various velocities as the charging distance is changed from 13.3 cm (EARC I), to 32.0 cm (maximum allowable). It should be noted that a peak sensitivity occures at different velocities as the charging distance increases. Table VII is a summary of the values of sensitivity and efficiency at these peak values of sensitivity. The results of Tables V and VI lead one to draw a number of interesting conclusions.

Table V
Precipitator Sensitivity (m^3/min) as a Function of
Velocity and Charging Distance

Velocity (cm/sec) \ Charging Distance (cm)	13.3	20.0	25.0	32.0
964	44.49	45.55	46.14	46.94
2000	75.37	78.46	80.29	82.90
5000	125.88	136.28	142.91	149.59
9000	148.25	168.98	181.72	195.58
11000	148.34	174.28	190.75	207.31
12000	144.45	174.58	191.85	212.04
13000	140.17	175.13	192.27	214.82
14000	136.22	171.65	192.92	215.32
16000	129.29	163.83	187.35	217.07
19000	120.70	153.85	176.71	207.04

Table VI
Precipitator Efficiency (%) as a Function of
Velocity and Charging Distance

Velocity (cm/sec) \ Charging Distance (cm)	13.3	20.0	25.0	32.0
964	92.55	94.76	95.97	97.63
2000	75.56	78.66	80.49	83.11
5000	50.47	54.64	57.30	59.98
9000	33.02	37.64	40.48	43.57
11000	27.07	31.76	34.76	37.78
12000	24.13	27.16	32.05	35.42
13000	21.61	27.01	29.65	33.13
14000	19.50	24.58	27.62	30.83
16000	16.20	20.53	23.47	27.20
19000	12.73	16.23	18.64	21.84

Table VII

Precipitator Values at Peak Sensitivity

DCH (cm)	VL (cm/sec)	EFF (%)	FQQ	CUR (amps/set)	SEN (m^3/min)
13.3	11000	27.03	.53	.00125	148.34
20.0	13000	27.01	.59	.00188	175.13
25.0	14000	27.62	.62	.00235	192.92
32.0	16000	27.20	.65	.00312	217.07

The upper limit of the charging distance is set by the power supply available. In this case, the sixteen sets of charging plates set an upper limit of 32 cm for the charging distance using a 50 ma power supply. This is true if the corona wires are spaced so that the current density is 3.62×10^{-6} amps/cm^2. A larger charging distance would require a larger power supply.

There is no significant gain in sensitivity as the charging distance is increased at low velocities (964 cm/sec). There is however, a significant increase in sensitivity as the charging distance is increased at the optimum velocity. The optimum velocity increases with an increase in charging distance. This may be especially valuable in airborne applications where a high velocity is required and easily provided.

The precipitator efficiency at peak sensitivity remains almost constant as the charging distance and velocity change. However it does increase as the charging distance increases if the velocity remains constant. The percent saturation charge by bombardment, FQQ, increases as the charging distance increases because of the longer time spent in the charging section by the particles.

The current per cathode-anode set increases as the charging distance is increased. A high current is desirable but may require a larger power supply. A larger power supply is the penalty a designer must pay if he wishes to increase the sensitivity by increasing the charging distance past 32.0 cm.

An interesting result that is not shown in Tables V and VI is that the maximum sensitivity in each case occurs at the velocity where the fraction of the largest group collected is just equal to 1.0, or in other words all of the largest size group particles are barely being collected.

Optimum Charging. The optimum parameters for the charging section have now been determined. It has been shown that for optimum charging and sensitivity, the values for the electric field (E), corona current (CUR), and the charging distance (DCH), must be as large as possible. The precipitator must also be operated at the optimum velocity to take advantage of the large values of voltage and corona current. The partially optimized precipitator now has the following values for its operating parameters:

E = 10850 volts/cm	VL = 16000 cm/sec
CUR = .00312 amps/set	FRAR = 832 cm^2
DCH = 32.0 cm	DL = 58.5 cm
SEPC = 2.0 cm	SEP = 2.0 cm
AREA = 837.2 cm^2	ECOL = 9000 volts/cm

If the precipitator were designed and operated under the above conditions (the collection section parameters are as previously specified) the predicted results would be as follows:

Volume flow - VOL	=	798.03	m^3/min
Sensitivity - SEN	=	217.07	m^3/min
Efficiency - EFF	=	27.20	%
Saturation chg - FQQ	=	65.0	%
Ion density - G	=	1.17×10^9	$ions/cm^3$
Charging time - T	=	.002	sec

Collection Section

The second precipitator stage to be optimized is the collection section. The charging section parameters will be held fixed during the optimization of the collection section. With fixed charging parameters, there are only a few parameters that may be varied in the collection section. These are the applied collection potential, flow velocity, collection length, and the collection plate separation distance. The collection length and separation distance will be optimized separately with the velocity changing in certain instances.

Specifications. The specifications of the collection section will include fixed parameters, and the limits that are imposed upon the ones that are to be varied. All charging section parameters will be held fixed except the velocity. It is assumed that the velocity is variable with no restrictions set on the upper limit. Although it may be possible to achieve a higher electric field between the collection plates than 9000 volts/cm, it is assumed that this value represents the upper limit, and therefore the electric field between the collection plates is held fixed at this value. The collector plate length (DL), is assumed variable up to a length of 300 cm. The limits on plate separation

are dictated by practicability. In other words there are only certain plate geometries that are practical when the charging plate separation distance is set at 2.0 cm.

Collection Length. As was mentioned in the specifications for the collection section, the collection length has an upper limit of 300 cm. The collection length will be varied from the EARC I value of 58.5 cm to the upper limit of 300 cm. The effect of increasing the collection length is somewhat intuitive. The fraction collected in the collection section for a plate separation distance of 2 cm is given by Eq (21) as

$$FC = \frac{DA}{(SEP - DAC)} \tag{21}$$

where FC is the fraction of the aerosols that leave the charging section that are collected in the collection section, DA is the distance these particles travel toward the anode in the collection section in cm, SEP is the distance between the collector plates in cm, and DAC is the distance traveled toward the anode by the particles while they were in the ionization section in cm. Increasing the collection length affects only the distance traveled toward the anode (DA) in Eq (21), therefore it is apparent that the fraction collected will increase with increasing collection length. The effects of increasing the collection length (DL), while holding all other parameters constant is presented in Table VIII. Precipitator parameters used in the calculation of Table VIII are the values stated under the optimum charging section except of course the collection length, which is variable. Table VIII

not only indicates the increasing trend in the sensitivity and efficiency, but it also shows that these values increase by a factor of about two as the collection length reaches the upper limits.

Table VIII

Sensitivity and Efficiency as a Function of Collection Length

Coll Length DL (cm)	Sensitivity SEN(m^3/min)	Efficiency EFF(%)
58.5	217.27	27.20
100.0	285.82	35.81
150.0	345.60	43.30
200.0	391.22	49.02
250.0	426.00	53.38
300.00	463.25	58.04

Collection Plate Separation Distance. Since the charging plate separation distance has been fixed at 2 cm,there are only two practical geometries that may be applied to the collection process. First, a geometry similar to the charging section geometry is applicable. That is to say a plate separation distance of 2 cm with the plates positioned similar to that of EARC I is applicable. Second, the plates may be positioned 1 cm apart with the negative plate placed between the two positive plates. Since the 2 cm plate separation has been considered throughout this thesis, the practicability of placing the plates 1 cm apart will now be considered.

Although the problem of spacing the collection plates 1 cm apart is not difficult, the computer collection theory is complex and all possible collection cases must be considered. The geometry

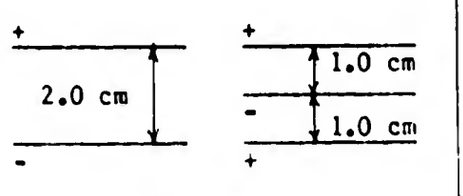

Figure 11

1.0 cm Collection Plate Geometry

to be considered is presented in Fig. 11. With the 1 cm geometry several assumptions are necessary. First the assumption is made that no current flows between any charging plate and any collection plate. This assumption is quite valid if the two sections are spaced properly and insulated in such a way so as to prevent arcing between the two sections.

The second assumption is that the particles achieve drift velocity instantaneously in the collection section. This assumption will be valid if the time it takes an aerosol to accelerate from a zero or small velocity to its drift velocity is small compared to the time spent in the collection section. Since a large particle accelerates slower than a small particle under the same force, an aerosol from the largest size group will be used in the calculations. The aerosol is conservatively assumed to have a density equal to that of water (1 gram/cm^3). The volume of an aerosol of any size group may be expressed as

$$V = \frac{4}{3}\pi r^3 \tag{32}$$

where r is the radius of the particle in cm. Therefore the volume of an aerosol whose radius is 8.5 microns is 2.59×10^{-9} cm^3. The mass of the particle is also equal to 2.59×10^{-9} grams. The force on the particle is given as

$$F = Fq - Fs \tag{33}$$

where Fq is the force due to the electric field in dynes and Fs is force on the particle according to Stokes' law in dynes. The sum of

these forces is equal to the mass of the particle multiplied by its acceleration or

$$Fq - Fs = m\frac{dv}{dt} \tag{34}$$

and upon substitution of Eq (16) and Eq (6) for Fq and Fs, and rearranging results in

$$\frac{dv}{dt} + C_1V = C_2 \tag{35}$$

where

$$C_1 = \frac{6\pi nr}{m} \tag{36}$$

$$C_2 = \frac{QQe\ ECOL}{m} \tag{37}$$

where n is the viscosity of the air in poise, ECOL is the electric field in volts/cm, m is the mass of the particle in grams, r is the particle radius in cm, QQ is the charged achieved by the particle while in the ionization section in electrons, and e is the charge on the electrons. The use of Laplace transforms (Ref 11:308) gives the solution to Eq (35) as

$$V(t) = \frac{C_2}{C_1}\ (1 - e^{-C_1t}) \tag{38}$$

where V(t) is the particle velocity as a function of time t in cm/sec. For air at 75°F and 1 atm the value of the viscosity is given as 1.8×10^{-4} poise (Ref 10:371). If the value of charge achieved is conservatively taken as 5×10^4 electrons, and the electric field is 9×10^3 volts/cm the values of C_1 and C_2 are calculated to be 1.11×10^3 sec^{-1} and 2.78×10^5 cm^{-1} respectively. Eq (38) indicates

that as the time approaches infinity, the terminal velocity approaches C_1/C_2 or 251 cm/sec. Since this velocity will never be reached, a more meaningful time might be the time to achieve 90% of the terminal velocity or 226 cm/sec. Upon substitution of this value for velocity into Eq (38) for V(t), the time is calculated to be 2×10^{-3} sec. Since this time is short compared to the time spent by the particle in the collection section (about 1×10^{-2} sec) the assumption made is justified.

The third assumption made is that the incoming particles are homogeneously distributed throughout the incoming air.

The 1 cm plate separation geometry lends itself nicely to a digital computer solution. The computer program used for the 2 cm plate separation (Appendix A) is not valid, and therefore a portion must be changed. The 1 cm collection plate theory will be presented for all possible collection cases as outlined in Fig. 12, and the combined program change is presented in Appendix B.

In the first case (Fig.12), the distance traveled by the particles while they are in the charging section is greater than the charging plate separation distance. This means simply that all of the particles are collected on the charging plate (FCC = 1.0), and none are collected in the collection section (FC = 0).

In the second case (Fig. 12), the distance traveled by the particles while they are in the charging section is less than the charging plate separation (2.0 cm) but greater than the collection plate separation (1.0 cm). In this case some of the particles will be collected in the charging section, the fraction being collected expressed by Eq (15) as

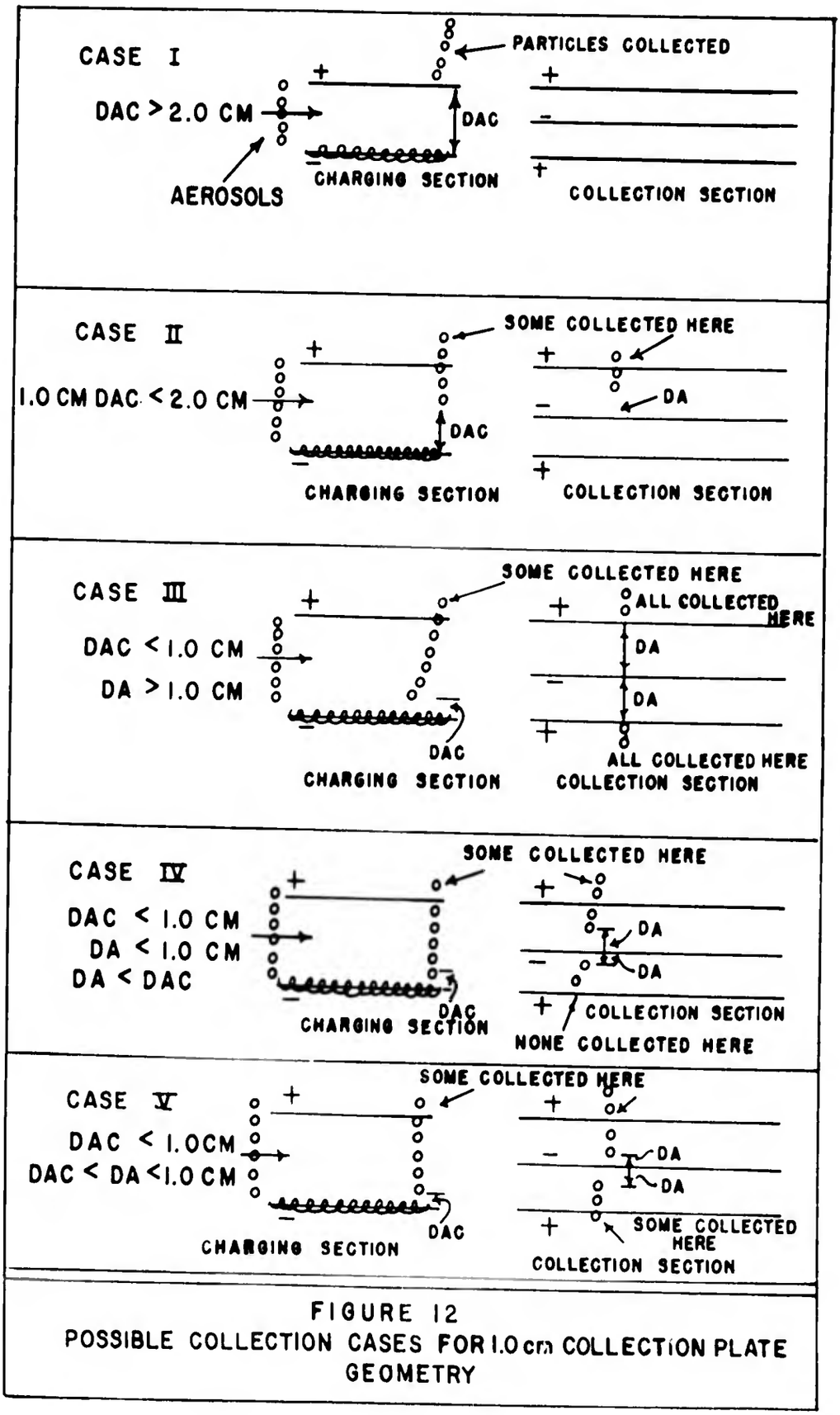

FIGURE 12
POSSIBLE COLLECTION CASES FOR 1.0 cm COLLECTION PLATE GEOMETRY

$$FCC = \frac{DAC}{SEPC} \tag{15}$$

where DAC is the vertical distance traveled by the particles while they are in the charging section in cm, and SEPC is the charging plate separation distance in cm. Some of the particles that are not collected in the charging section are collected on the upper plate in the collection section, and this fraction may be expressed as

$$FC = \frac{DA}{(2.0 - DAC)} \tag{39}$$

where DA is the distance traveled toward the collection anode in cm, and DAC is the distance traveled by the particles while they are in the ionization section.

In the third case (Fig. 12), the distance traveled by the particles while they are in the ionization section is less than the collection plate separation distance, and the distance traveled by the particles after they enter the collection section is greater than the collection plate separation distance (1.0 cm). In this case the fraction collected in the charging section may again be expressed by Eq (15) and the fraction collected in the collection section is equal to 1.0.

In the fourth case (Fig. 12), the distance traveled by the particles while they are being charged is less than the collection plate separation distance but greater than the distance traveled by the particles after they enter the collection section. Also, the distance traveled in the collection section is less than the collection plate separation distance. The fraction collected in the charging section

may again be expressed by Eq (15), and the fraction collected in the collection section is again equal to Eq (35). No particles are collected in the lower collection section.

In the last case (Fig. 12), the distance traveled by the particles in the charging section is less than the collection plate separation distance. The distance traveled by the particles in the collection section is greater than the distance traveled by the particles in the charging section, but less than the collection plate separation distance. In this case the fraction of the particles collected in the charging section may once more be calculated by Eq (15), but the fraction collected in the collection section must be divided into a fraction collected in the upper section (FCU), and a fraction collected in the lower section (FCL). The values of the fractions collected in the upper and lower sections may be calculated by

$$FCU = \frac{DA}{(2.0 - DAC)} \tag{40}$$

and

$$FCL = \frac{(DA - DAC)}{(2.0 - DAC)} \tag{41}$$

where DA and DAC are the distances traveled by the particles in the collection and charging sections respectively. The fraction collected in the combined upper and lower sections is

$$FC = FCU + FCL \tag{42}$$

The total fraction collected in the precipitation process is again expressed by Eq (22) as

$$FRTO = FCC + (1 - FCC)\, FC \qquad (22)$$

where FCC and FC are the fractions collected in the charging and collecting sections respectively. All possible cases have now been considered.

The effects of a 1 cm plate separation will now be studied using the parameters of the optimum charging section. The collection length will again be varied from 58.5 cm to the upper limit of 300 cm. That is to say that the precipitator has the same operating parameters used in calculating Table VIII except that the collection plate separation distance is now 1 cm. Table IX shows the results of such a calculation.

Table IX

Sensitivity and Efficiency as a Function of Collection Length

Length DL(cm)	Sensitivity SEN(m^3/min)	Efficiency EFF(%)
58.5	271.77	34.05
100.0	367.37	46.03
150.0	442.96	55.50
200.0	495.29	62.06
250.0	536.93	61.28
300.0	569.41	71.31

Velocity Effects. Tables VIII and IX show that a long collection length is desirable, and therefore this parameter will be fixed at the upper limit of 300 cm. The value of velocity (16000 cm/sec) used in the calculation of Tables VIII and IX is no longer the optimum velocity, since the collection length has been changed from the original 58.5 cm. Therefore the optimum velocity will once more be determined for both collection plate separation distances with a collection length of

Table X
Precipitator Efficiency and Sensitivity as a Function of Flow Velocity with a 1.0 cm Collection Plate Separation

Velocity (cm/sec)	Sensitivity (m^3/min)	Efficiency (%)
10000	421.02	84.41
12000	475.55	79.45
14000	525.74	75.28
16000	569.41	71.35
18000	611.33	68.09
20000	644.84	64.64
22000	678.88	61.86
24000	713.51	59.60
26000	738.31	56.93
28000	759.28	54.36
30000	780.90	52.18
32000	803.19	50.32
34000	819.07	48.29
36000	832.45	46.36
38000	846.15	44.64
40000	860.75	43.14
42000	873.43	41.69
44000	878.02	40.00
46000	883.36	38.50
48000	888.62	37.11
50000	894.67	35.87
52000	901.40	34.75
55000	900.49	32.82

Table XI
Precipitator Efficiency and Sensitivity as a Function of Flow Velocity with a 2.0 cm Collection Plate Separation

Velocity (cm/sec)	Sensitivity (m^3/min)	Efficiency (%)
10000	354.68	71.11
12000	394.68	65.94
14000	430.87	61.70
16000	463.25	58.04
18000	485.78	54.10
20000	508.95	51.02
22000	527.81	48.10
24000	542.60	45.32
26000	557.99	43.02
28000	568.82	40.73
30000	574.99	38.42
32000	581.81	36.45
34000	588.96	34.73
36000	589.45	32.82
38000	587.58	31.00
40000	586.71	29.40
42000	585.87	27.96

300 cm. The results of these calculations are presented in Tables X and XI. These results show that the optimum velocity for each case is quite different. Previously it was stated that the velocity had no upper limits. At this point an upper limit of the speed of sound will be placed on the velocity. The speed of sound at sea level is 34500 cm/sec (Ref 9:3375), therefore the limiting velocity is now fixed at 34000 cm/sec, a value slightly lower than the speed of sound.

The upper limit of the flow velocity is lower than the calculated optimum velocity for both collection plate separation distances. Therefore, the sensitivities must be compared at the 34000 cm/sec velocity instead of the optimum velocity. Table X lists the results of the important data for the two plate separation distances at a velocity of 34000 cm/sec.

The Optimum

Table XII shows that a large gain in sensitivity will result if the collection plates are placed 1 cm apart. Therefore, the optimum precipitator will have collection plates that are 1 cm apart. At this point the results of the optimum precipitator will be presented. The operating parameters of the optimum precipitator, as well as a simplified drawing of the optimum design is presented in Fig. 13. The optimum results are presented in Table XIII.

Table XII

Sensitivity and Efficiency as a Function of Plate Separation

Separation SEP(cm)	Sensitivity SEN(m^3/min)	Efficiency EFF(%)
1	819.07	48.29
2	588.96	34.73

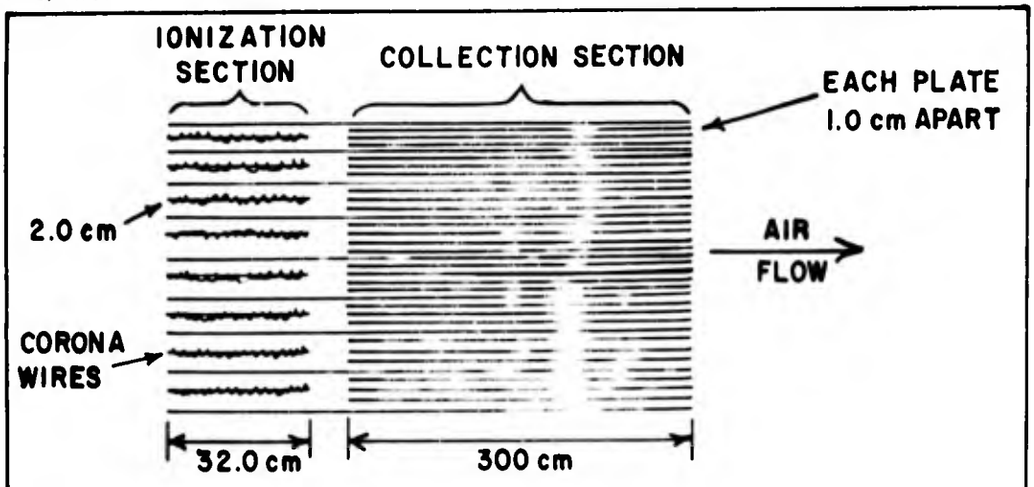

SIDE VIEW CROSS SECTION

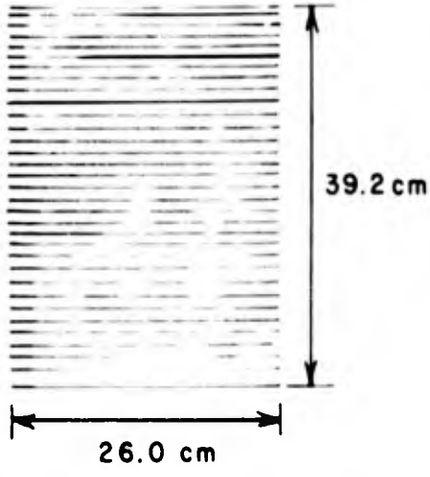

FRONT VIEW

OPERATING PARAMETERS

E = 10850 volts / cm	VL = 34000 cm / sec
CUR = .00312 amps	FRAR = 832 cm^2
DCH = 32.0 cm	DL = 300 cm
SEPC = 2.0 cm	SEP = 1.0 cm
AREA = 837.2 cm^2	ECOL = 9000 volts/cm

FIGURE 13

THE OPTIMUM PRECIPITATOR

Table XIII
Computed Results for the Optimum Precipitator

Size Group	Avg Radius (u)	Charge Achieved (electrons)	Total Fraction Collected
1	.125	1	.07
2	.200	3	.09
3	.300	7	.12
4	.425	145	.16
5	.600	290	.21
6	.850	583	.29
7	1.250	1261	.41
8	2.000	3229	.64
9	3.000	7267	.94
10	4.250	14584	1.00
11	6.000	29069	1.00
12	8.500	58339	1.00

Volume Flow (m^3/min)	Sensitivity (m^3/min)	Efficiency (%)
1695.85	819.07	48.29

Ion Density (ions/cm^3)	Corona Current (amps)	Saturation Chg (%)
1.2×10^9	3.12×10^{-3}	47.74

Summary

This entire chapter has been devoted to the optimization of a two stage parallel-plate precipitator. It is well to consider in retrospect the material that has been presented and the important conclusions that may be drawn from the results.

A change in any one of many variable parameters will result in a change in sensitivity and efficiency. It was determined that although a high charging voltage and corona current are always desirable, these high values are especially important when the precipitator is operating at the optimum velocity. A large charging distance is also desirable, and the maximum charging distance is dependent upon the power supply selected. This is true assuming the corona wire geometry remains the same at the same time the charging distance is increased. This leads one to conclude that after a power supply has been selected, the designer should determine the proper charging length so as to fully utilize all of the corona current available. This task may take a combination of experimental and theoretical calculations.

The effects of collection plate length and separation distance were investigated. The results indicate that a long collection length is advantageous. The facilities available to the operator for the removal of dust from the plates may dictate the plate length.

The utilization of the 1 cm collection plate geometry indicates that a significant gain in sensitivity and efficiency over the 2 cm plate geometry is available. The 1 cm plate separation calculations resulted in an increase of sensitivity of 230.11 m^3/min and an efficiency increase of 13.56% over the 2 cm plate geometry. The added plates do not represent an added cleaning problem as they do not

collect the negatively charged particles. The collection section optimization was completed by once again changing the velocity while holding all the other parameters fixed.

An upper limit was placed on the velocity because the optimum velocity was found to be greater than the speed of sound for both collection plate geometries. The effects of shock waves have not been considered, therefore the upper limit of the velocity was set at a value slightly lower than the speed of sound at sea level.

The optimum precipitator is one that fully utilizes the alloted space and the selected power supply. It has been demonstrated that the optimum precipitator that would fit into a volume 26 cm wide, 39.2 cm high, and 300 cm in length, utilizing a 50 ma power supply would have a sensitivity of 819.07 m^3/min. This value is about 20 times higher than the calculated sensitivity of EARC I, and around 800 times higher than the Staplex high volume air sampler. The efficiency of the optimum precipitator (48.29%) however, is about half the calculated efficiency of EARC I (92.55%).

It should be remembered that the optimum design presented is operating at a very high flow velocity (34000 cm/sec), and the effects of turbulence and re-entrainment have not been considered. Table XIII shows that only .07 of the smallest size group particles are collected. Although this figure seems small when compared to the .56 value for EARC I, the optimum precipitator actually collects more m^3/min of the smallest size group than EARC I. This is true because of the much higher flow rate that is available to the optimum design.

The effects of the parameters that were varied should aid the precipitator designer throughout the entire precipitator design stage, and the use of the computer programs presented should give the designer some idea of what to expect in the way of results.

In conclusion, the results predicted for the optimum precipitator are very attractive. The results however, are purely theoretical and can only be validated by a wind tunnel analysis of such a configuration. The next logical step therefore, is to present a design that would be tested at these high velocities to determine the feasibility of the optimum design.

V. Precipitator Design

Design Objectives

The previous chapter indicated a requirement for high flow velocities; therefore the purpose of this chapter is to design a two-stage parallel plate precipitator in order to determine the feasibility of collecting radioactive aerosols at high velocities and altitudes. With this purpose in mind, the design will be preliminary in nature and therefore simple and straightforward. The design is not intended to be mounted in an aircraft, but is to be tested in a wind tunnel. When built, the precipitator would be capable of determining if a corona discharge can be maintained at high velocities and altitudes. Also, if the corona discharge can be maintained, would the sensitivity of the precipitator be sufficient to determine the amount of radioactivity present, and therefore justify the application of a aircraft mounted precipitator.

The optimum design presented in Chapter IV predicts a high sensitivity (819.07 m^3/min) at a velocity very near the speed of sound at sea level. This high sensitivity resulted when the effects of turbulence and re-entrainment were neglected. Only if the design were built and tested at these high velocities can these effects be fully understood. The design presented in this chapter will be a small scale precipitator. In other words it will consist of only one segment of charging and collection plates.

With the purpose of this chapter in mind, the precipitator design must accomplish the following objectives:

1. The precipitator must be compact and simple in construction.
2. The predicted results from the design must show a sensitivity of at least 50 m^3/min.

Charging Section

Since the corona current and corresponding electric field can only be determined experimentally, certain assumptions must be made. First, it is assumed that the current density in the charging section is the same as that of EARC I. This should be true if the design uses the same type wire and has the same wire geometry and plate spacing. Second, it is assumed that the effective ionization field is equal to 10350 volts/cm. This assumption should be conservative if the current per wire-plate set is equal to, or greater than the value given for EARC I (1.25×10^{-3} amps).

Geometry. The geometry of the charging section necessarily limits the geometry of the collection section. Since the design is to be tested in a wind tunnel it must be compact. The charging section therefore, is to consist of one aluminum corona wire frame and two aluminum collection plates spaced 2 cm on each side of the corona wires.

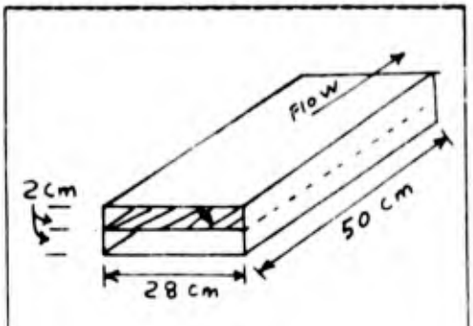

Figure 14

Charging Section

The charging section plates will be independent of the collection plates because it is anticipated that a very small percentage of the particles will be collected in the charging section. The plates will be removable however, so that they may be cleaned if necessary.

Since the design is to consist of only one segment of plates and wires, the total current used in the charging section should not require a large power supply. The results of Chapter IV indicate that a plate width of 26 cm and a charging length of 50 cm should be adequate. A simple sketch of the charging section is presented in Fig. 14.

Both the length of the charging section and the velocities anticipated indicate that the corona wires will require additional support on the aluminum frame. A detailed drawing of the corona wire frame is presented in Fig. 15. A 1 cm edge on each side of the frame is included in the design for mounting purposes. As can be seen from Fig. 15, the longest distance between the supports is about 12 cm.

Corona Current. Since the current density, with the wires placed as shown in Fig. 15 is assumed to be 3.62×10^{-6} amps/cm^2, the current per cathode-anode set may be easily calculated. The area of the corona wire cathode is

$$\text{Area} = (26 \text{ cm})(50 \text{ cm})$$
$$= 1300 \text{ cm}^2$$

If the current density is

$$\frac{\text{CUR}}{\text{AREA}} = 3.62 \times 10^{-6} \text{ amps/cm}^2$$

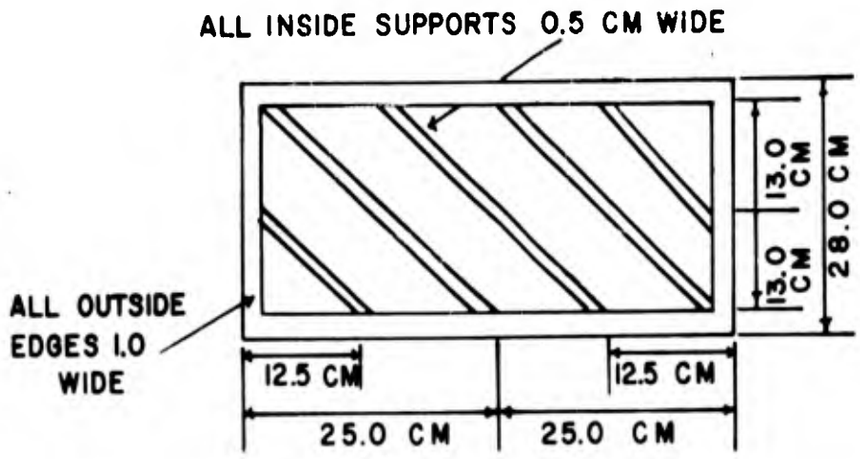

TOP VIEW— FRAME WITHOUT WIRES

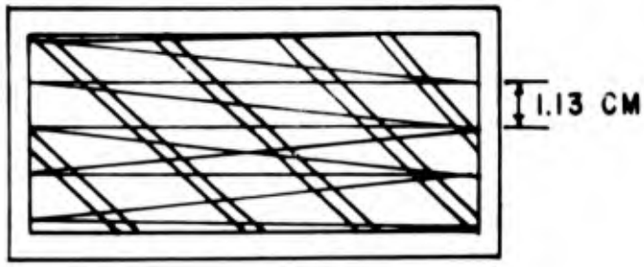

FRAME WITH 23 TURNS OF .5 MIL.
TUNGSTEN CORONA WIRE SPACED 1.13 CM APART.

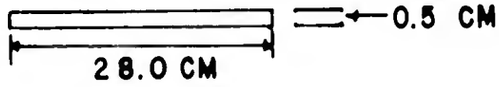

FRONT VIEW

FIGURE 15

CHARGING SECTION CATHODE

then the current per cathode-anode set is

$$CUR = (3.62 \times 10^{-6} \text{ amps/cm}^2)(1.3 \times 10^{3} \text{cm}^2)$$
$$= 4.70 \times 10^{-3} \text{ amps}$$

This current is shared by the wire cathode and one plate, therefore, the total current (I) is just twice the stated value, or 9.4×10^{-3} amps. Therefore, a power supply with a current rating of 10 ma and 22 kv will be sufficient for the operation of the design.

Collection Section

The design goals call for a compact precipitator that will have a sensitivity of at least 50 m^3/min. The results of Chapter IV indicates that the optimum velocity increases as the collection length is increased. Since a velocity of around 34000 cm/sec is desired, the collection length should be such that the optimum velocity is as close as possible to this figure. The scope of this thesis, however, does not allow a thorough optimization of this parameter.

Geometry. The results of Chapter IV indicate that a collection plate separation distance of 1 cm is desirable, and that a collection length of 150 cm would be adequate to meet the design goals. A simple sketch of the collection section is presented in Fig. 16. The plates are to be fabricated of

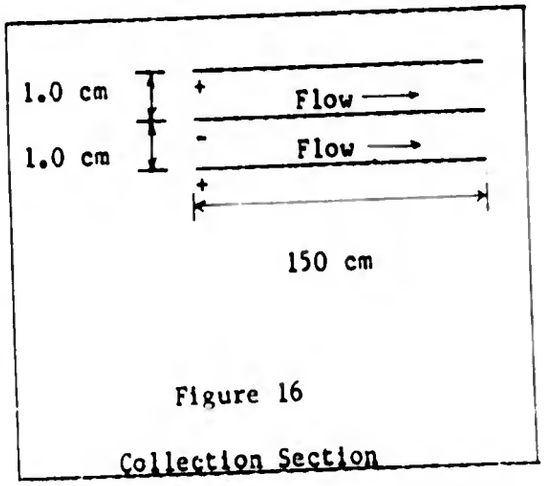

Figure 16

Collection Section

0.5 cm polished aluminum 150 cm long and 28 cm wide. The plates will extend 1 cm into the sides of the precipitator frame.

Electric Field. Although the operator of the designed precipitator should strive to achieve the maximum voltage potential across the collection plates, the collection field is assumed to be 9000 volts/cm. This value is used because experimental results (Ref 3:Chapter III) indicate that 9000 volts/cm will not cause arcing.

Combined Charging and Collection Sections

The charging and collection sections have been presented separately. The design will be complete after the two sections are mounted in a suitable frame. The frame is to be fabricated of 4 cm thick plexiglass. The charging and collection plates will be separated by 6 cm of air. Figure 17 is a simplified drawing of the assembled precipitator. This figure is not intended to be a working drawing, but it is detailed enough for a preliminary design.

Operating Parameters. The operating parameters of the design are now fixed with the exception of the velocity which is variable. The fixed parameters are as follows:

E	= 10850	volts/cm	FRAR	= 104	cm^2
CUR	= .0047	amps	DL	= 150	cm
DCH	= 50	cm	SEP	= 1.0	cm
AREA	= 1300	cm^2	ECOL	= 9000	volts/cm
SEPC	= 2.0	cm			

Although the velocity is variable, one of the goals of the design is to test the precipitator at velocities very near the speed of sound at sea level.

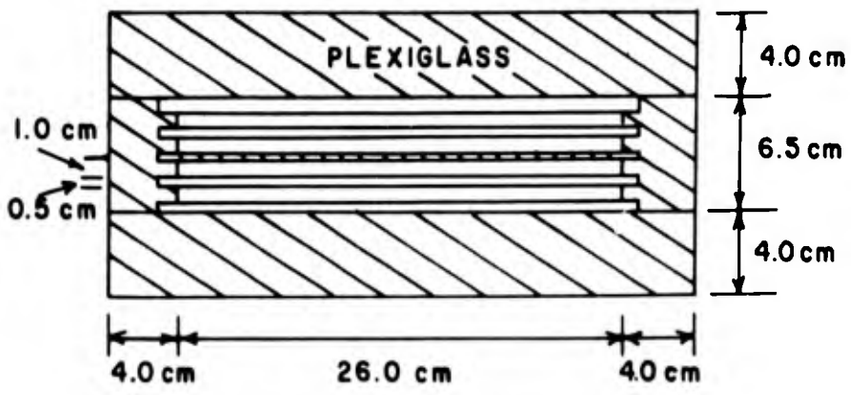

FRONT VIEW

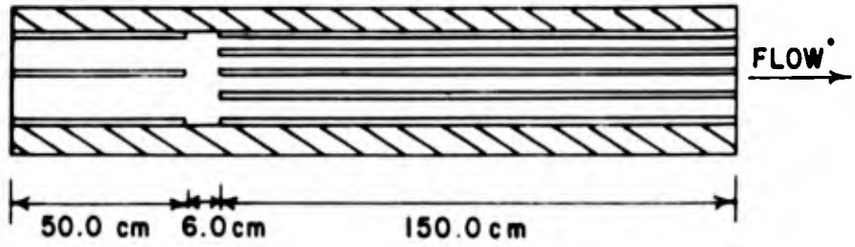

SIDE VIEW CROSS SECTION

FIGURE 17

COMBINED CHARGING & COLLECTION SECTIONS

Optimum Velocity. It has been shown that a change in sensitivity will result if the velocity is changed. The ideal results that one might expect from any precipitator design is for the peak sensitivity to occur at the exact design velocity. Therefore, it is necessary to determine the velocity where the peak sensitivity occurs. The design velocity was varied from 10000 cm/sec to 39000 cm/sec, a value slightly greater than the speed of sound at sea level. The predicted sensitivities and efficiencies as a function of velocity are presented in Table XIV.

Results

Table XIV shows that the optimum velocity is 36000 cm/sec. This value is larger than the speed of sound at sea level, and therefore the design velocity must be restricted to 34000 cm/sec as an upper limit. The predicted sensitivity of the design at a velocity of 34000 cm/sec is 75.89 m^3/min. This value is only .98 m^3/min less than the optimum sensitivity. The corresponding efficiency at a velocity of 34000 cm/sec is calculated to be 35.77%.

The results indicate that the precipitator may be operated at any velocity between 13000 cm/sec and the upper limit of 34000 cm/sec and still achieve the design goal of 50 m^3/min sensitivity.

Table XV is a summary of results for the 34000 cm/sec operating condition. These results show that the fraction of particles collected in the charging section range from .006 for the group 1 particles to .226 for the group 12 particles.

Table XIV
Sensitivity and Efficiency as a Function of Velocity

Velocity (cm/sec)	Sensitivity (m^3/min)	Efficiency (%)
10000	44.08	70.64
11000	46.87	68.29
12000	49.16	65.66
13000	51.47	63.45
14000	53.78	61.56
15000	56.10	59.93
16000	58.14	58.24
17000	59.64	56.22
18000	61.16	54.45
19000	62.68	52.87
20000	64.22	51.46
21000	65.77	50.19
22000	66.98	48.79
23000	67.98	47.36
24000	68.99	46.06
25000	70.01	44.88
26000	71.04	43.79
27000	72.09	42.78
28000	73.06	41.81
29000	73.49	40.61
30000	73.95	39.50
31000	74.42	38.47
32000	74.89	37.50
33000	75.39	36.61
34000	75.89	35.77
35000	76.40	34.98
36000	76.87	34.22
37000	76.79	33.26
38000	76.74	32.36
39000	76.69	31.51

Table XV
Predicted Design Results at a
Velocity of 34000 cm/sec

Size Group	Fractions Collected			Charge Achieved (electrons)
	Charging	Collection	Total	
1	.006	.03	.04	1
2	.008	.04	.05	3
3	.010	.06	.07	8
4	.014	.08	.09	168
5	.018	.10	.12	336
6	.025	.14	.17	675
7	.035	.21	.23	1461
8	.055	.33	.37	3741
9	.082	.50	.54	8418
10	.115	.73	.76	16895
11	.161	1.00	1.00	33673
12	.226	1.00	1.00	67580

Sensitivity	=	75.89 m^3/min
Efficiency	=	35.77 %
Volume Flow	=	212.16 m^3/min
Corona Current	=	4.7×10^{-3} amps
Time	=	.0014 sec
Ion Density	=	1.17×10^9 ion /cm^3
% Saturation Chg	=	58.07 %

Summary and Conclusions

The purpose of this chapter was to present a precipitator design to be tested in a wind tunnel at high velocities. The design was to be compact and yet achieve a sensitivity of at least 50 m^3/min. These two design goals were achieved.

The design drawings were not intended to be working drawings. Although the measurements are stated, the builder of the design may find it necessary to improvise in certain places. For instance it may be necessary to increase the distance between the charging and collecting plates to prevent arcing at that point. The charging section should be built and tested under static conditions to determine the true corona current and electric field present between the wires and plates.

The predicted sensitivity is about 25 m^3/min higher than the design goal. This is somewhat analogous to a safety factor of 50 %. In other words if, because of turbulence and re-entrainment, the precipitator loses one third of the particles that are predicted to be collected, the remaining particles will more than satisfy the counting requirements.

VI. Summary of Conclusions

The purpose of this thesis has been threefold. The first main topic presented was the analysis of the two stage parallel plate precipitator named EARC I. With the aid of values of operating parameters obtained from EARC I data, the next topic discussed was the optimization of a two-stage parallel-plate precipitator. The last topic presented was a proposed design to be built and tested in a high speed wind tunnel. The goal of this thesis is to establish ideas of design philosophy in order to aid designers of future precipitators. The conclusions of this study will be summarized in the same pattern as the topics were presented.

The purpose of the analysis of EARC I was twofold. First, it was necessary to theoretically predict the results achieved by EARC I. Second, it was desirable to determine what effects on sensitivity might be expected if certain parameters were varied. It is concluded that it is possible to increase the sensitivity of EARC I fourfold if the operating velocity is increased to 11000 cm/sec. It is also concluded that a high corona current and field strength is desirable but not critical at the low operating velocity at which EARC I is operating. This conclusion is very important as it infers that the operating power conditions may be lowered somewhat without lowering the sensitivity prohibitively. It also infers that the charging section of EARC I is overdesigned in comparison with the flow velocity available. Further, it is concluded that the sensitivity (44.49 m^3/min) of EARC I

represents a significant increase over the Staplex high volume filter system (1 m^3/min). The final conclusion made concerning EARC I is that the smallest size group particles (.125 u) are the hardest to collect and that the four largest size group particles (3.0 - 8.5 u) are collected in the charging section.

The purpose of the precipitator optimization chapter was to study the effects of varying the parameters involved in the precipitation process, and to optimize a two-stage electrostatic precipitator. The results were intended to aid future designers of precipitators in understanding the effects of varying the many parameters present. The calculations resulted in many interesting conclusions. First, it is concluded that a high current and electric field is always desirable, and are especially advantageous if the precipitator is operating at, or near, the optimum velocity. It is also concluded that a large charging distance is desirable, and this distance should be large enough to fully utilize the power supply available. This conclusion is important in that the charging length is limited by the power supply available, and care must be taken so that the charging section will not be "under-designed". The conclusion is also made that the collection section length should be as long as practicable, and that a collection geometry such as the 1.0 cm geometry is highly advantageous. It is further concluded that changing the flow velocity will result in a significant change in precipitator sensitivity, and a peak sensitivity will occur at some velocity if all other parameters are held constant. The final conclusion made concerning precipitator optimization is that it is theoretically possible to achieve a sensitivity of 819.07 m^3/min using

a precipitator that is only 26 cm wide, 39.2 cm high and 300 cm in length. This conclusion is perhaps the most important one resulting from this thesis. In effect, this conclusion demonstrates the theoretical usefulness of the electrostatic precipitator as a means of sampling airborne radioactivity.

The purpose of the precipitator design chapter was to design a two-stage parallel-plate precipitator in order to determine the feasibility of collecting radioactive aerosols at high velocities and altitudes. The design calculations produced interesting results which foster the following conclusions. First, it is concluded that a compact, efficient precipitator is theoretically feasible. It is further concluded that the presented design will theoretically have a high enough sensitivity (75.89 m^3/min) to insure satisfactory radioactivity analysis of airborne aerosols.

Finally, it is concluded that the role of the electrostatic precipitator in the field of nuclear engineering has been firmly established, and that the feasibility of using electrostatic precipitation as a method of collecting radioactive aerosols has been demonstrated.

VII. Recommendations for Future Action

The results of this thesis indicate that several areas of precipitator theory should be further investigated. Therefore, the following recommendations for future investigation are submitted. Recommendation (1) should be considered before the design is tested, and recommendations (3) and (4) should be investigated after the fabricated design is in operation.

1. The relationship between corona current and applied potential in the charging section should be investigated in detail. This study should include the effects of increasing the charging length while the corona wire geometry remains constant.
2. The precipitator design presented in Chapter V should be fabricated and tested in a high speed wind tunnel. The wind tunnel tests should determine if it is possible to achieve a corona discharge at high velocities and altitudes. The tests should also determine whether or not the sensitivity of the design is sufficient to insure satisfactory radiation analysis.
3. The theory presented in Chapter II should be validated by experimental techniques. This might be accomplished by verification of the predicted sensitivity using a filter comparison test.

4. The effects of turbulence and re-entrainment on precipitator sensitivity should be investigated over the complete velocity range. (0-34,500 cm/sec).

Bibliography

1. Baker, John W. Sampling of Airborne Radioactive Particles by Electrostatic Precipitation. M. S. Thesis, Institute of Technology, Air University, Wright-Patterson Air Force Base, Ohio, 1962.

2. Handbook of Chemistry and Physics (Forty-First Edition). Cleveland, Ohio: Chemical Rubber Publishing Co., 1960.

3. Kennard, E. H. Kinetic Theory of Gases. New York: McGraw-Hill Book Co., Inc., 1938.

4. Lamberson, D. L. A Study of the Electrostatic Precipitation of Radioactive Aerosols. M. S. Thesis, Institute of Technology, Air University, Wright-Patterson Air Force Base, Ohio, 1961.

5. Orr, C., and Dallavalle, J. M. Fine Particle Measurement. New York: The MacMillan Company, 1959.

6. Penny, G. W., and Matick, R. E. "Potential in D-C Corona Fields". Transactions: American Institute of Electrical Engineers, Communications and Electronics-Part I, 79:91-99 (May 1960).

7. Perry, John H. (Editor). Chemical Engineering Handbook (Third Edition). New York: McGraw-Hill Book Co., Inc., 1950.

8. Rose, H. E., and Wood, A. J. An Introduction to Electrostatic Precipitation in Theory and Practice. London: Constable & Company LTD., 1956.

9. Sangren, Ward C. Digital Computers and Nuclear Reactor Calculations. New York: John Wiley & Sons, Inc., 1960.

10. White, H. J. "Particle Charging in Electrostatic Precipitation." Transactions: American Institute of Electrical Engineers-Part II, 70:1186-1191 (1951).

11. Wylie, C. R. Jr. Advanced Engineering Mathematics. New York: McGraw-Hill Book Co., Inc., 1960.

Appendix A

Digital Computer Solution for Precipitator Sensitivity and Efficiency for a 2.0 cm Collection Plate Geometry

General

As was previously mentioned, the calculated results throughout this thesis were obtained from a computer program written in Fortran language and entered into an IBM 7090 Digital Computer. The purpose of this Appendix is to present the program that was used, and to explain the programs use and limitations. A basic knowledge of computer programming is assumed. This Appendix will be divided into three sections. First, the program will be presented, after which its limitations and utilization procedures will be discussed.

Program

The complete program for the solution of precipitator sensitivity and efficiency with a collection plate separation distance of 2.0 cm is as follows:

```
*61-323         690   3  O.S. STUART
*      XEQ
       DIMENSION Q(1001),R(12),CUN(12),FR(12),V(1001),FRC(12)
100    FORMAT(E11.4)
101    FORMAT(613)
103    FORMAT(1P2E24.7)
105    FORMAT(50X,4HQQ =1PE15.7,10X,6HFRTO =0PF15.7)
106    FORMAT(30X,4HFC =F15.7,10X,5HFCC =F15.7)
107    FORMAT(1HO,49X,5HSEN =F15.7,9X,3HT =F15.7)
108    FORMAT(1HO,3HG =1PE20.7,26X,5HVOL =1PE15.7,10X,5HEFF =E15.7,5X,
      15HFQQ =0PF8.5)
109    FORMAT(1PE30.7)
1      READ INPUT TAPE 2, 101,IJ,IK
```

```
2     READ INPUT TAPE 2,100,(R(J),J=1,12),(CUN(J),J=1,12),(FR(J),J=1,
     112)
      DO 102 JJ= 1,IJ
3     READ INPUT TAPE 2,100,VL,SEP,DL,DCH,SEPC,FRAR,E,CUR,AREA,ECOL
      J = 1
      DELT = 0.0001
      VLCL=VL
      G =(.352E19*CUR)/(E*AREA)
4     H= G*R(J)**2.*E
      A = 11.16*H
      B = 2.*A*7.203E-8/(E*R(J)**2.)
      C = B*7.203E-8/(2.*E*R(J)**2.)
      D = 15.7E4*G*R(J)**2.
      F = 5.56E-6/R(J)
      T = DCH/VL
      IT = ((T/DELT) + 1.0) +0.0001
      I = 1
      Q(I) = 0.
5     XYZ = F*Q(I)
      IF(XYZ-87.4)9,9,7
7     QP = A-B*Q(I) + C*Q(I)*Q(I)
      GO TO 15
9     IF(XYZ-.00001) 11,11,13
11    QP = A-B*Q(I)+C*Q(I)*Q(I) + D
      GO TO 15
13    QP = A - B*Q(I) + C*Q(I)*Q(I) + D*EXPF(-XYZ)
15    I = I + 1
      IF(I-1001)17,17,20
17    Q(I) = Q(I-1)+ QP*DELT
      GO TO 5
20    T = 0.
      IF(IK)25,99,25
99    DO 130 I = 1,1001,10
      WRITE OUTPUT TAPE3,103,Q(I),T
130   T= T + DELT*10.
25    T=DCH/VL
      I = (T/DELT) + 1.
      Y = Q(I+1) - Q(I)
      U = I - 1
      U = U*DELT
      X = T-U
      DB = Y*X/DELT
35    QQ = Q(I) + DB
      DAC = 0
      DO 55 I=1,IT
      V(I) = 1.602E-12*Q(I)*E*CUN(J)/(6. *3.1416*1.8E-04*R(J))
55    DAC = DAC + (V(I)*DELT)
88    VTER = 1.602E-12*QQ*E*CUN(J)/(6.0*3.1416*1.8E-04*R(J))
999   DAC = DAC + (VTER*X)
      FCC = DAC/SEPC
      IF(FCC-1.0)122,111,111
```

```
111   FCC = 1.0
122   VD = 4.73E-10*QQ*ECOL*CUN(J)/R(J)
      DA=VD*DL/VLCL
      IF(FCC-1.0)30,29,29
29    FC = 0.
      GO TO 45
30    FC = DA/(SEP-DAC)
      IF(FC - 1.)45,45,38
38    FC = 1.
45    WRITEOUTPUT TAPE 3, 106,FC,FCC
      FRTO = FCC + ((1.0-FCC)*FC)
       WRITE OUTPUT TAPE3,105,QQ,FRTO
      FRC(J) = FR(J)*FRTO
      J=J+1
      IF(J-12) 4,4,50
50    J=1
      SEN=FRC(J)*VL*FRAR
      J=J+1
52     SEN = (SEN + FRC(J)*VL*FRAR)
      J=J+1
      IF(J-12) 52,52,60
60    SEN = SEN*60./1.E6
      WRITE OUTPUT TAPE 3,109,CUR
      WRITE OUTPUT TAPE3,107,SEN,T
      VOL = VL*FRAR*6.0000E-05
      EFF = SEN/VOL
      FQQ = 1.0/(1.0+(1.0/(8.03E-07*G*T)))
102   WRITE OUTPUT TAPE3,108,G,VOL,EFF,FQQ
      CALL EXIT
      END
*     DATA
```

Limitations

The limitations of the preceeding program will now be discussed. First, the program is applicable only for a two-stage parallel-plate precipitator, and the relation between the geometry of the collection section plates and the ionization section plates must be similar to that of EARC I. That is to say, the anode of both the charging section and collection sections must be positioned in the same horizontal plane.

The numerical analysis solution of Eq (4) results in 1001 values of charge (Q(I)) for 1001 values of time (T) at .0001 sec intervals.

It is required to obtain a value of charge achieved (QQ) for the time (T) that the particle is in the ionization section. The time that the particle spends in the ionisation section is equal to the charging length (DCH) divided by flow velocity (VL). Since this value of time will probably fall between two computed values of Q(I) vs T, it is necessary to interpolate to determine the charge actually achieved. This interpolation process begins with statement number 25 and ends with statement number 35. This program will give values of charge (Q(I)) for times of 0 sec to .1001 sec at .0001 sec intervals. The limitation is that the value of T (DCH divided by VL) must not be less than .0001 sec or more than .1 sec. If the time (T) lies outside this range, the program cannot perform the interpolation process, and an error will result.

Utilization Procedures

The utilization procedures for the computer program presented is simple and straightforward. There are three sets of IBM cards that must be inserted after the "Data" card at the end of the program. The first set consists of only one card. This card satisfies IJ and IK in statement number 1. The number of computations (one set of parameters constitutes one computation) are placed in the first two columns of the card. If twenty sets of parameters are to be computed, the number 20 is punched in the first two spaces of the card. If it is not desired to print out values of charge Q(I) vs time (T), a number (any number) is placed in either column 3, 4, or 5 on the same card. These spaces are left blank if these values are desired. The next set,

consisting of 36 cards, is placed immediately after the "number of computations" card. These 36 cards represent the input data cards for statement number 2. The last set of data cards is the ten cards which represent the precipitator operating parameters as outlined in statement number 3. Care must be taken to insure that these cards are placed in the proper sequence.

The program is designed to compute and print values of all fractions collected by each size group particle. The charge achieved by each size particle, as well as the time the particles spend in the charging section, is printed. The fraction of bombardment saturation charge, ion density, precipitator sensitivity, efficiency, and volume flow of air are also printed as computer output.

Appendix B

Computer Program Correction for a 1.0 cm Collection Plate Separation Distance

The computer program as outlined in Appendix A of this thesis must be corrected if the distance between collection plates is 1.0 cm. This correction is also necessary if the relative geometry of the ionization and collection plates is similar to that of the precipitator presented in Chapter V. That is to say, the fact that the collection plate separation distance is 1.0 cm, is not the influencing factor. However, the relative geometries of the ionization and collection section plates necessitate the program change.

The alteration amounts to all statements (Appendix A) between statement number 999 and statement number 45 inclusive be replaced by:

```
999   DAC = DAC + (VTER*X)
122   VD = 4.73E-10*QQ*ECOL*CUN(J)/R(J)
      DA = VD*DL/VLCL
      IF(DAC-2.0)200,300,300
300   FCC=1.0
      FC=0.
      GO TO 45
200   FCC = DAC/SEPC
      IF(DAC-1.0)500,700,700
500   FCU =DA/1.0
      IF(FCU-1.0)600,800,800
800   FCU = 1.0
600   IF(DA-1.0)6000,620,620
620   FCL=1.0
      FC=1.0
      GO TO 45
6000  IF(DA-DAC)550,770,770
550   FCL=0.0
      FC =FCU
```

```
      GO TO 45
770   FCU = DA/(2.0-DAC)
      FCL = (DA-DAC)/(2.0-DAC)
      FC = FCU + FCL
      IF(FC-1.0)1010,1020,1020
1020  FC = 1.0
1010  GO TO 45
700   FC = DA/(2.0-DAC)
      IF(FC-1.0)45,860,860
860   FC = 1.0
45    WRITEOUTPUT TAPE 3, 106,FC,FCC
```

The same program limitations and utilization procedures outlined in Appendix A are applicable in this case.

Vita

Robert Stanley Stuart was born in [redacted] to Edwin R. Stuart and Angelyn G. Stuart. The Stuart family moved to [redacted]. After completion of high school at [redacted], he was enrolled in the School of Engineering at Texas A & M College, College Station, Texas. He was commissioned a Second Lieutenant in the United States Air Force Reserve concurrently with receiving the degree of Bachelor of Science in Aeronautical Engineering from Texas A & M in 1957. He immediately entered the Air Force and was assigned as Aircraft Maintenance Officer at Sembach Air Base, Germany, with the United States Air Forces in Europe. Immediately prior to his present assignment at the Institute of Technology, Air University, he was a Detachment Commander of a Special Weapon Bombing Range with the United States Air Forces in Europe.

Permanent Address: [redacted]

This thesis was typed by Mrs. Frances L. Athey.

UNCLASSIFIED